Climate Services 30 (2023) 100388

Contents lists available at ScienceDirect

Climate Services

journal homepage: www.elsevier.com/locate/cliser

Hydrological modeling of spatial and temporal variations in streamflow due to multiple climate change scenarios in northwestern Morocco

Siham Acharki [a], Soufiane Taia [b], Youssef Arjdal [b], Jochen Hack [c,*]

[a] Department of Earth Sciences, Faculty of Sciences and Technologies of Tangier (FSTT), Abdelmalek Essaadi University, Tetouan 93000, Morocco
[b] Natural Resources & Sustainable development Laboratory, Earth Sciences Department, Faculty of Sciences, Ibn Tofail University, Kenitra 14000, Morocco
[c] Institute of Environmental Planning, Leibniz University Hannover, 30419 Hannover, Germany

HIGHLIGHTS

- SWAT model was calibrated and validated in Loukkos basin.
- RCM/GCM models anticipated an increase in average minimum and maximum temperatures.
- Future projection would exhibit a decrease in precipitation, with few exceptions.
- Future streamflow was projected under two RCPs/SSPs scenarios.
- Climate change will have an impact on annual and seasonal streamflow, particularly from 2071–2100.

GRAPHICAL ABSTRACT

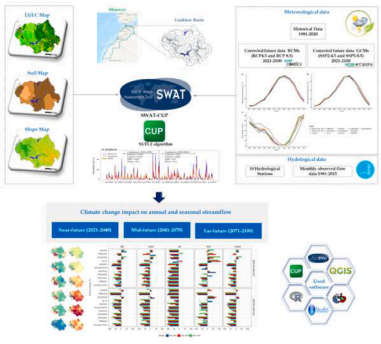

ARTICLE INFO

Keywords:
Climate change
Sentinel-2
SWAT model
Streamflow
CMIP6

ABSTRACT

Climate change is one of the most important factors impacting hydrological regimes. In this paper, climate change impact on streamflow of Loukkos basin (northwestern Morocco) is evaluated using SWAT model for three future periods: near (2021–2040), mid (2041–2070), and far (2071–2100), compared to baseline 1981–2020. A set of bias-corrected climate models was used: five regional climate models (EURO-CORDEX), four global climate models (CMIP6) and their ensemble mean, under two representative concentration pathways respectively (RCP 4.5; RCP 8.5) and (SSP2-4.5; SSP5-8.5). Furthermore, SUFI-2 algorithm in SWAT-CUP was performed to calibrate (1981–1997), validate (1998–2015), and analyze uncertainty for each dataset at ten hydrological stations. In most stations, statistical performance indicated a good simulation, with a Nash–Sutcliffe efficiency (NSE) greater than 0.77 and percent bias (PBIAS) within ±10% on a monthly basis. Overall, 82% of models indicated that future climate could decline streamflow. The largest decrease would be for 2071–2100 and under RCP 8.5/SSP5-8.5. Our findings could help planners and policymakers in developing reasonable water management policies and climate change adaptation measures.

* Corresponding author.
E-mail address: hack@umwelt.uni-hannover.de (J. Hack).

https://doi.org/10.1016/j.cliser.2023.100388

Available online 18 May 2023

Practical implications

Morocco, as one of the most Mediterranean and North African countries, has experienced several frequent drought episodes induced by a decrease in precipitation and a significant increase in temperature over the last decades (Driouech et al., 2020; Verner et al., 2018). According to Toreti et al. (2022), the country is currently experiencing its worst drought in three decades. Such changes could have serious implications for water resources, agriculture, hydropower production, and a variety of socioeconomic sectors. Due to this rapidly intensifying climate change, decision-makers now require more detailed and precise information. Thus, climate modeling and services continue to pique researcher's interest, owing to their importance in guiding policies and other societal actions aimed at mitigating and adapting to climate change, as well as making society more resilient to climatic risks (Hewitt et al., 2021).

To prepare for and adapt to a changing climate, climate change impacts need to be defined. In addition, to investigate the hydrological impact of climate change, researchers commonly run hydrological models with climate projections, which are typically provided by climate model outputs for interest areas (Jose and Dwarakish, 2020). Therefore, scientists employ hydrological modeling in conjunction with future projected climate from GCMs and/or Regional Climate Models (RCMs).

In this context, this paper aims to develop robust and reliable information on streamflow climate change impact on a Mediterranean coastal watershed. Such information can be used to size optimal adaptation decisions water resource sector. Furthermore, it can be extremely beneficial for other socio-economic sectors that are affected by climate variability. Therefore, the simulated conditions must be appropriate for the hydrological problem addressed. In this study, we project future climate impact scenarios on streamflows using hydrological model (SWAT), and the climate services of four CMIP5-based models RCMs and five CMIP6-based models GCMs (and their ensemble means).

Introduction

Climate change's effects have multiplied and become more frequent, affecting all natural systems (IPCC, 2021; Acharki, 2020; Tramblay et al., 2018). Therefore, all societal sectors, including water management, are impeded as a result of these effects. Recently, to support climate change mitigation and adaptation, there has been an increase in demand for useful and usable climate information, as well as an adapted infrastructure known as "climate services" (Larsen et al., 2021; Hewitt et al., 2021; Donnelly et al., 2018; van den Hurk et al., 2018). Climate information is defined as longer-term risk profiling requiring data over decades (Georgeson et al., 2017). According to Hewitt and Stone (2021), a climate service may be defined as the provision of climate information for use in decision-making. Climate data and services provide a wide range of information sources, such as basic climate data, climate change scenarios and projections, vulnerability studies, socioeconomic indicators related to climate change, and climate change education and training (Larsen et al., 2021). For instance, for water-related climate services, each service offers varying ensembles of global and regional circulation models (RCMs and GCMs), as well as a selection of emissions scenarios (RCPs) to drive one or more different hydrological models (Donnelly et al., 2018). Furthermore, van den Hurk et al. (2018) highlighted that most services rely on more sources of climate information than climate model outputs.

The Sixth Assessment Report (AR6) of the Intergovernmental Panel on Climate Change (IPCC, 2021) predicts an increase in average temperatures (between 1.5 °C and 4 °C) and a decrease in precipitation (between 4% and 27%) over the Mediterranean region including North Africa. Additionally, the IPCC (2021) noted an observed and projected increase in dry climatic impact-drivers (aridity, hydrological, agricultural and ecological droughts, and fire weather). Therefore, a significant increase in temperature would have a significant impact on a region's water resources. Besides, numerous studies (Tramblay et al., 2018; Guo et al., 2020; Gebrechorkos et al., 2020; IPCC, 2021) highlighted that climate change is anticipated to have a net negative impact on water resources in almost every part of the world. In the Mediterranean region, which is considered as a hotspot of climate change (IPCC, 2021), several studies (Meddi and Eslamian, 2021; Sinan and Belhouji, 2016) have confirmed a decline in water resources in recent decades. They also predict that the Mediterranean region will be inevitably subjected to a future potential decrease in water resources (López-Ballesteros et al., 2020; Mami et al., 2021; Martínez-Salvador et al., 2021; Saade et al., 2021; Tramblay et al., 2018; Pulido-Velazquez et al., 2021).

In order to assess and quantify future hydrologic responses to climate change, scientists employ hydrologic modeling in conjunction with future projected climate produced from General Circulation Models (GCMs) and/or Regional Climate Models (RCMs) (Quansah et al., 2021). In fact, GCMs provide reliable climate information, that is required to support mitigation policies, on global and large regional scales, covering a huge and diverse environment (Fang et al., 2015; Lee et al., 2019; Raju and Kumar, 2020; IPCC, 2021). Regional climate models, with a higher spatial resolution, have been established to resolve the heterogeneity of diverse geographical regions in a very efficient manner, alleviating the uncertainty of GCMs (Lee et al., 2019). Several researchers (Luo et al., 2018; Tramblay et al., 2018) highlighted that RCMs provide more suitable climate information on smaller scales. Furthermore, RCMs/GCMs climate model outputs and knowledge gained from them form the scientific basis for climate services, which are designed to provide tailored information to decision-makers and policymakers (Hewitt and Stone, 2021; Hewitt et al., 2021; van den Hurk et al., 2018). However, global and regional climate model projections still contain significant biases, which is inherited through GCM forcing or caused by systematic model errors that lead to inconsistencies between models (Martínez-Salvador et al., 2021; Teutschbein and Seibert, 2012). For this reason, bias correction of RCM/GCM data is required before using the data in any climate change effects investigation (Luo et al., 2018). Various bias correction methods have been developed (e.g., linear scaling, local intensity scaling, power transformation, distribution mapping, and quantile mapping). They have been advocated to minimize differences between observed and simulated values of climate variables (Awotwi et al., 2021; Brouziyne et al., 2020; Fang et al., 2015; Lee et al., 2019; Luo et al., 2018; Mami et al., 2021; Martínez-Salvador et al., 2021; Teutschbein and Seibert, 2012).

Currently, the Coupled Model Intercomparison Project Phase 6 (CMIP6) dataset is the most recent GCM dataset. This dataset differs from CMIP3 and CMIP5 datasets in terms of forcing scenarios and carbon emissions, in addition to a better representation of physical processes (Bourdeau-Goulet and Hassanzadeh, 2021). A new set of Shared Socioeconomic Pathway (SSP) scenarios is used (O'Neill et al., 2017). Historical data and predictions based on several SSP scenarios are included in CMIP6 data, which are compatible with CMIP3 and CMIP5 Representative Concentration Pathways (RCPs) (van Vuuren et al., 2011) via shared policy assumptions. CMIP6 improves upon CMIP5 with more modeling groups, experiments, scenarios, and some advancements in current climate simulation, including increased spatial resolution (Grose et al., 2020; Di Virgilio et al., 2022). According to Zhu and Yang (2020) and Fan et al. (2020), the benefits of using CMIP6 models rather than CMIP5 models are especially apparent when investigating climatic extremes. Several studies have been conducted using CMIP6 climate model data to assess future temperature and precipitation changes and the reliability of climate predictions in sub-regions of the Mediterranean region and Morocco (Bouramdane, 2022; Majdi et al., 2022; Hamed et al., 2022). Their results indicated that GCMs from CMIP6 exhibited a noteworthy enhancement in their performance, specifically in simulating the climate over the region, resulting in a reduction in uncertainty when compared to their CMIP5 counterparts. Nevertheless, there is still a need for research focusing on the potential impact of climate change

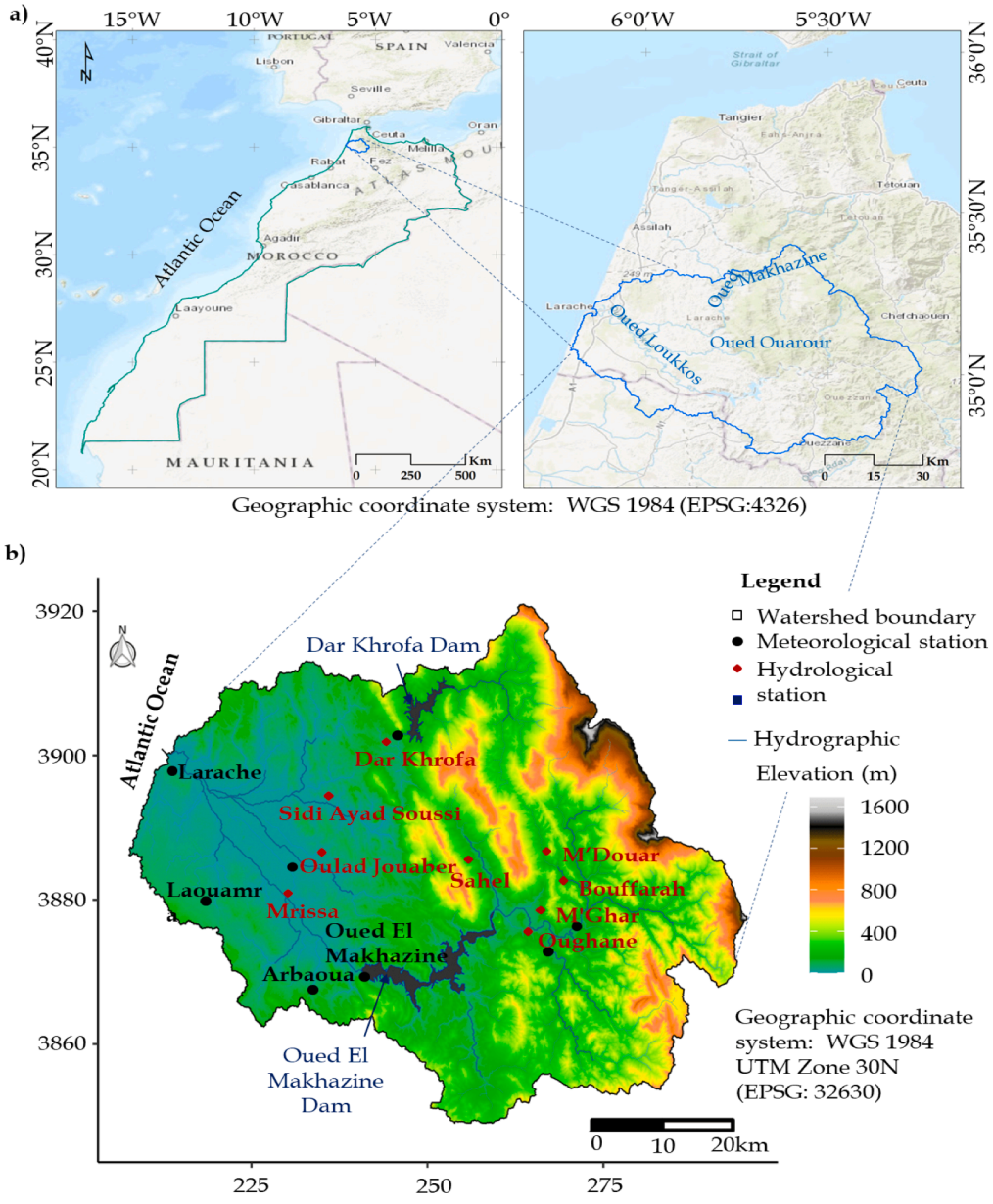

Fig. 1. a) Location map of the Loukkos basin in Morocco. b) Digital Elevation Model, hydrographic network, location of meteorological and hydrological stations of the Loukkos basin.

on hydrologic processes. Testing and evaluating the uncertainty of CMIP6 when predicting streamflow can provide additional information to stockholders and decision-makers.

In the context of hydrological modelling, a wide range of models have been embraced by researchers, including SWAT (e.g., (Milewski et al., 2019)), GR2M (e.g., (El Khalki et al., 2021)), GR4J (e.g., (Tramblay et al., 2013)), GUO-5P (e.g., (Pulido-Velazquez et al., 2021)), 2CAFDYM (e.g., (Acharki, 2020)) and HEC-HMS (e.g., (Candela et al., 2016)). Among these models, the Soil and Water Assessment Tool (Arnold et al., 1998), which is a conceptual model with a semi-distributed physical base, has been widely applied around the world (Aghsaei et al., 2020; Awotwi et al., 2021; Bal et al., 2021; Brouziyne et al., 2018; Gebrechorkos et al., 2020; Guo et al., 2020; Lee et al., 2019; Choto and Fetene, 2019; Nilawar and Waikar, 2019; Quansah et al., 2021; Saade et al., 2021; Nyatuame et al., 2020). Generally, this model has demonstrated his efficiency in hydrological assessments (Aghsaei et al., 2020; Awotwi et al., 2021). Furthermore, SWAT allows for long-term climate change implications on water (e.g., (Gemechu et al., 2021)), sediment (e.g., (Choto and Fetene, 2019)), and nutrient loads (e.g., (Mehan et al., 2019)) in catchments with varying topography, land use, soils, and management conditions.

Several studies were conducted across the Mediterranean region to examine climate and LULC change's impact on watershed hydrology under different climate models and scenarios using different hydrological models (Choukri et al., 2020; Moçayd et al., 2020; López-Ballesteros et al., 2020; Mami et al., 2021; Marchane et al., 2017; Martínez-Salvador et al., 2021; Milewski et al., 2019; Saade et al., 2021; Tramblay et al., 2018; Pulido-Velazquez et al., 2021). López-Ballesteros et al. (2020) have combined the SWAT model with IAHRIS software and five GCMs from ISI-MIP5 to assess climate change impact on the hydrological regime of Aracthos River (North-western Greece). This study indicates a reduction in streamflow by 20%. Using sixteen regional climate models from EURO-CORDEX and SWAT hydrological model, Martínez-Salvador et al. (2021) reported reductions from 46.3% to 55.8% in future streamflow of two semi-arid catchments in Spain. They also imply that one of the most likely outcomes of climate change will be the occurrence

of more intense and long-lasting droughts over time. Saade et al. (2021) investigated climate change impact, using REMO 2009 and SWAT model, on the El Kalb river's streamflow (Lebanon) and indicated that streamflow will reduce by 23% to 45%. They concluded that, during 2061–2080 and under RCP 8.5, mean annual temperatures are anticipated to rise 2.75 °C and mean annual precipitation to fall 40.6%, reducing streamflow from 5.47 m^3/s to 2.98 m^3/s (45.5% decrease). Similarly, Mami et al. (2021) evaluated hydrological response to climate change projections in Algeria (Tafna basin). Their results were analyzed using a combination of eight GCMs, two RCMs from CORDEX-Africa (RCA4 and CCLM4-8–17), under RCPs 4.5 and 8.5, and the SWAT model. For the projected period 2020–2099, they predict a decrease in surface flow (from 20% to 48%) and river discharge (between 42% and 54%), as a consequence of reduced precipitation. In Morocco, like other countries around the Mediterranean, climate change has a direct impact on water resources, with a considerable declining trend in surface water resources. Although various research on climate change have been conducted in Morocco (Driouech, 2010; Driouech et al., 2020; Filahi et al., 2017; Marchane et al., 2017; Tramblay et al., 2013) only limited studies have investigated multiple RCMs and/or GCMs dataset (Moçayd et al., 2020; Milewski et al., 2019; El Khalki et al., 2021; Babaousmail et al., 2022). No studies, so far, have used GCMs of CMIP6 to assess possible future climate change on hydrologic processes.

The Loukkos basin, located in northwestern Morocco, has been identified as one of Morocco's most important agricultural and wettest basins. It is also well-known for its role in economic and social development. In addition, its surface water resources reached approximately 3.4 billion m^3/year (UNECE, 2021). It is, indeed, a water-rich watershed, with an average annual runoff of 1 km^3/year (Moçayd et al., 2020). However, the basin's water availability has reduced considerably during the last several decades (Moçayd et al., 2020; Acharki, 2020; Meddi and Eslamian, 2021). This, combined with the increasing population and expanding agricultural development activities, could lead to devastating water shortages in the future. Acharki (2020) assessed climate change impact on water resources in the upstream Loukkos basin (Loukkos perimeter) based on the 2CAFDYM model and reported that future annual surface water will drop by 9.2 to 25.5% from 2021 to 2050. However, in this previous work, measured streamflow was not taken into account for calibration and validation. In addition, it only employed one climate model using A1B scenario. Furthermore, the LULC map used as the input model had a spatial resolution of 30 m and was limited to six classes. Hence, it is essential to analyze multiple climate models and to evaluate future climate change impacts on streamflow for Loukkos basin. This study aims to provide more robust and reliable information of climate change's impact on streamflow in the Loukkos basin, a Mediterranean coastal watershed. This information will aid stakeholders in the water resource sector in making well-informed decisions regarding optimal adaptation strategies. Climate change's impact on Loukkos streamflow has specific implications for different stakeholders. For instance, Loukkos agricultural stakeholders require information regarding water availability changes and their impact on crop yields and irrigation practices. To make informed choices, these stakeholders need guidance on how to adapt, including transitioning to crops that require less water or adopting more efficient irrigation practices. Similarly, Loukkos' water resource managers are vital stakeholders who need guidance on managing water resources in a sustainable and equitable manner, considering the projected changes in water availability and the likelihood of water shortages. Additionally, this information can be beneficial for other socio-economic sectors that are affected by climate variability. Hence, this study's results will enable local and regional actors to better understand how streamflow will change in Loukkos basin under various climate change scenarios. As well as act as a reference for building future adaptation approaches for improved water management and development planning.

Given the aforementioned context, the main objectives of this study are to: (i) calibrate and validate a SWAT model for ten hydrological stations at monthly time steps and evaluate model performance; (ii) assess future climate changes using five RCMs from Euro-CORDEX, four GCMs of CMIP6 and their ensemble mean, under two RCPs and SSPs and three periods compared to the baseline period 1981–2020; (iii) quantify hydrological processes using a SWAT model for future climate scenarios; and (iv) investigate possible effects of climate changes on future streamflow in three periods: near (2021–2040), mid (2041–2070), and far (2071–2100) futures.

Methods and materials

Study area

The Loukkos basin (Fig. 1) is located in northwestern Morocco. It is one of Morocco's most important agricultural basins and has an area of about 3,761.5 km^2. In the west, the basin has flat plains with a relatively attenuated topography (less than 100 m). In the east, the terrain is mountainous with an altitude reaching 1677 m and an average altitude of 266 m. Geologically, the Loukkos basin is part of the Rif chain, which is located at the Apennine-Maghrebian Belt's western extremity. It is also characterized by a succession of Upper Cretaceous marl and shale, partially detached from Lower Cretaceous rocks (Martín-Martín et al., 2020). Globally, this basin has Mediterranean weather features, with a wet season (November to April) and a dry season (May to October). The average annual precipitation recorded at eight weather stations (Fig. 1) is 655.4 mm (73% fall in winter and autumn). The average annual minimum temperature is 13.1 °C and the average annual maximum temperature is 23.6 °C over the last four decades. The study area has a decreasing precipitation gradient from west to east, which reflects the continentality effect. According to a study by Moçayd et al. (2020), annual precipitation can approach 1,400 mm in some years leading to large interannual variability in runoff. The largest superficial water resource in the Loukkos basin is Oued Loukkos, which drains a portion of western slopes of Rif mountains and runs into the Atlantic Ocean. Its hydrographic network is mainly separated into three sub-basins: Loukkos, which drains an area of 2,100 km^2; Ouarour, which drains 620 km^2 in central part; and Makhazine, which drains an area of 880 km^2 in northern part (Pravema, 2012). The main dams are: (1) Oued El Makhazine dam, one of the Loukkos' most important affluents, which has a capacity of around 726 Mm^3 (Moçayd et al., 2020; Tramblay et al., 2013). It became operational in 1979 with four purposes: (i) hydroelectric power generation, (ii) water supply to urban areas, (iii) irrigation of more than 30,393 ha, and (iv) flood-control (Tramblay et al., 2013). (2) Dar Khrofa dam has a capacity of 480 Mm^3.

It serves to regulate water flows of approximately 140 Mm^3 per year and to irrigate about 21,000 hectares of agricultural land. (3) Loukkos Guard dam, located on the river's last stretch, maintains the necessary water level for good pumping conditions for agriculture purposes by preventing seawater intrusion (Pravema, 2012).

Data and sources

The climate change's impact on streamflow in Loukkos basin was simulated with the Soil and Water Assessment Tool version 2012 (SWAT; Arnold et al. (1998)), which requires a diversity of information related to meteorology, land use, soil, and agriculture. Although we used the SWAT 2012 version in our study, it is worth noting that a newer version of SWAT (SWAT+) has recently become available (Bieger et al., 2017). SWAT + can depict spatial representations more efficiently, and it also comprises modular codes specifically designed to support non-expert users in developing and utilizing the software for future purposes (Arnold et al., 2018). However, it is still being determined from the literature research whether this difference significantly impacts the accuracy of streamflow simulations. Given the suitability of SWAT 2012 in many regions (Taia et al., 2023; Echogdali et al., 2022; Erraioui et al., 2023), we believe that SWAT 2012 was sufficient and met our analysis

Table 1
Description of SWAT input data sources and their spatial resolution.

Inputs variables	Description	Spatial resolution	Source
DEM	Shuttle Radar Topography Mission (SRTM) (2011)	30 m × 30 m	United States Geological Survey (USGS)
Land use	Sentinel-2 data classified for land use (2020)	10 m × 10 m	This current study
Soil data	Food and Agriculture		
Organization (FAO) Soil map	1:1,000,000	FAO	
Meteorological data	Precipitation daily data (mm)	Station point data	Loukkos Hydraulic Basin Agency (ABHL) and Loukkos Regional Agricultural Development Office (ORMVAL)
	Daily data of minimum temperature (°C) and maximum temperature (°C)	Station point data	Climate Forecast System
Reanalysis (CFSR) and NASA–POWER			
Climate projection	Daily data of precipitation (mm), minimum temperature (°C) and maximum temperature (°C)	~12.5 km	
See Table 2 (EUR–11) and CMIP6	Euro-CORDEX		
Hydrological data	Daily average flow (m^3/s)	Station point data	ABHL

needs. SWAT input data used in this research, including variable type, source and spatial resolution are listed in Table 1 and described in the following subsections. The methodological approach adopted in this research is illustrated in Fig. 2.

Meteorological and hydrological data

a. Historical meteorological and hydrological data

Observed daily precipitation data acquired from Loukkos Hydraulic Basin Agency (ABHL) and Loukkos Regional Agricultural Development Office (ORMVAL) were used for the baseline period of 1981–2020. Only stations with years of continuous records were evaluated among the thirteen available weather stations. A total of eight weather stations located within the basin were considered (Fig. 1). Due to lack of or inability to access data for other weather variables, daily data for minimum and maximum air temperature were obtained from the National Centers for Environmental Prediction Climate Forecast System Reanalysis (NCEP/CSFR) for the period 1981–2014, and the Prediction of Worldwide Energy Resource dataset from the National Aeronautics and Space Administration (NASA–POWER) until 2020. CSFR and NASA–-POWER were chosen because of their high spatial resolution and the availability of meteorological variables that could be exploited over the long-term. Several studies (e.g., Bui et al. (2021) have found that CFSR data performs well in hydro-meteorological simulations around the world. In Morocco, Lagrini et al. (2020) used 927 stations of CSFR against 26 meteorological stations and proposed their utility for climate change projections. In Brazil, Monteiro et al. (2018) compared NASA–POWER data to observed data from 302 weather stations. Their results proved that NASA–POWER data performed better at greater latitudes and altitudes. They also suggest that these data might be used as a reliable source of climatic data for agricultural activities at regional and national scales.

Daily streamflow data were obtained from gaging reports provided by Loukkos Hydraulic Basin Agency for the period of 1981–2015. Ten hydrological stations were chosen to adequately represent the study basin, as illustrated in Fig. 1. To calibrate and validate the SWAT reservoir simulation, observed daily inflows from reservoir water

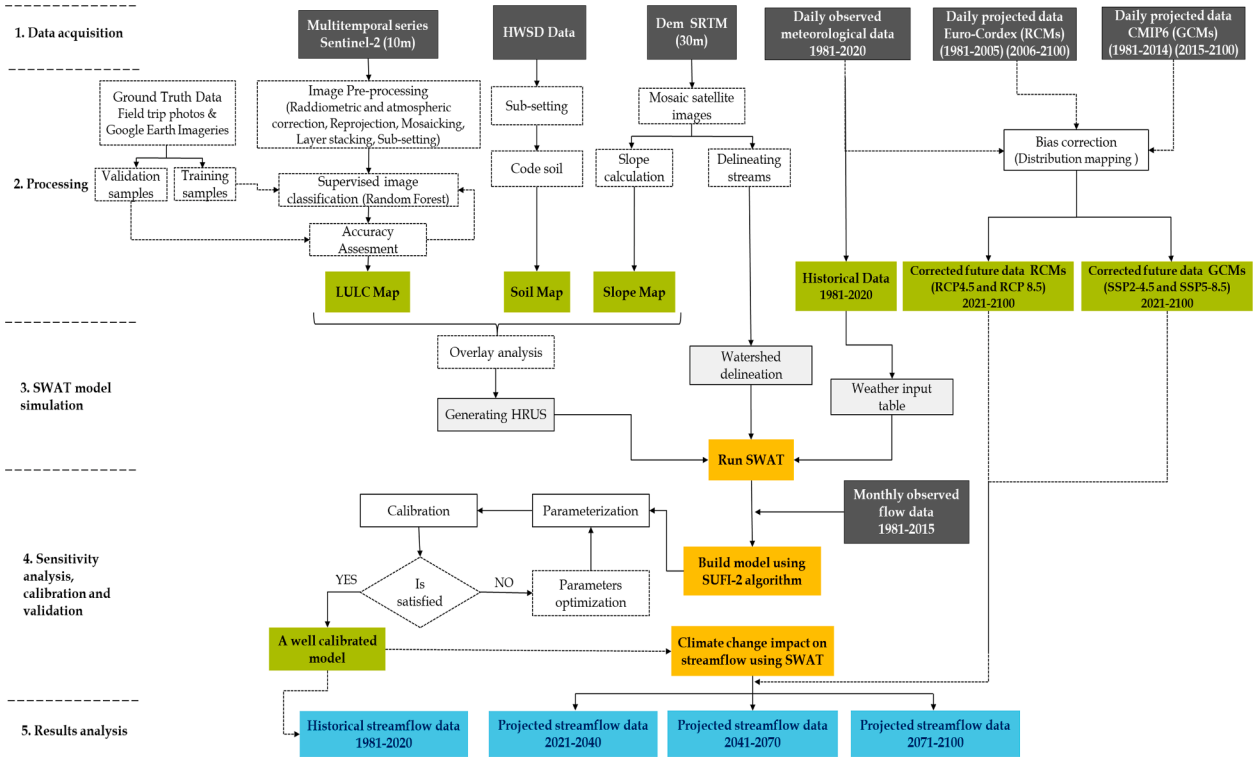

Fig. 2. Flow chart of methodology.

Table 2
List of selected GCMs and RCMs.

Model Type	Name	Variant	Institution	Spatial Resolution	Reference
RCM	ALADIN63_v2 (CNRM-CM5)	r1i1p1	Météo-France/Centre National de Recherches Météorologiques	0.11° × 0.11°	(Daniel et al., 2018)
RCM	HIRHAM5_v3 (NCC-NorESM1 -M)	r1i1p1	Danish Meteorological Institute	0.11° × 0.11°	(Christensen et al., 2007)
RCM	RACMO22E_v2 (CNRM-CM5)	r1i1p1	Royal Netherlands Meteorological Institute	0.11° × 0.11°	(van Meijgaard et al., 2012; van Meijgaard et al., 2008)
RCM	RCA4 (NCC-NorESM1-M)	r1i1p1	Swedish Meteorological and Hydrological Institute	0.11° × 0.11°	(Samuelsson et al., 2015; Strandberg et al., 2014)
RCM	WRF381P_v1 (CM5A-MR)	r1i1p1	Institut Pierre–Simon Laplace	0.11° × 0.11°	(Skamarock et al., 2008)
GCM	EC-Earth3-veg	r1i1p1f1	EC–EARTH consortium	0.7° × 0.7°	(Döscher et al., YYYY)
GCM	GFDL-ESM4	r1i1p1f1	NOAA Geophysical Fluid Dynamics Laboratory	1° × 1.25°	(Dunne et al., 2020; Guo et al., 2018)
GCM	IPSL-CM6A-LR	r1i1p1f1	Institut Pierre–Simon Laplace, France	1.26° × 2.5°	(Boucher et al., 2018; Boucher et al., 2020)
GCM	MPI-ESM-1–2-HR	r1i1p1f1	Max Planck Institute for Meteorology, Germany	0.93° × 0.93°	(Müller et al., 2018; von Storch et al., 2017)

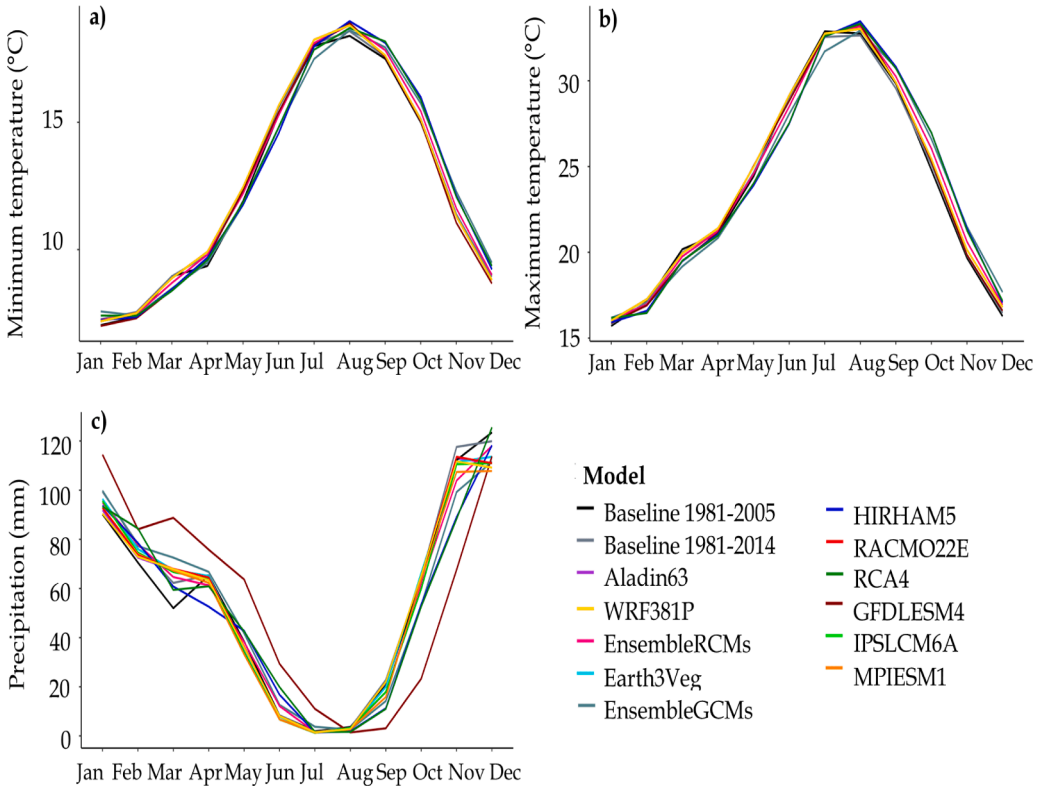

Fig. 3. Annual cycle of a) minimum temperature, b) maximum temperature and c) precipitation over Loukkos basin.

balance provided by ABHL were also used.

b. Projected meteorological data

Daily climate projections of precipitation, minimum and maximum temperature were obtained from eleven climate models: (i) five Regional Climate Models (RCMs) of the EURO-CORDEX initiative with a resolution of $0.11^{?} \times 0.11^{?}$ (~ 12.5 km × 12.5 km); (ii) four General Circulation Models (GCMs) of CMIP6 with varying resolution; (iii) an ensemble mean simulation of five RCMs and (iv) an ensemble mean simulation of four GCMs. These models were downloaded from the website of the Earth System Grid Federation (ESGF) (https://cordex.org/data-access/esgf/; https://esgf-node.llnl.gov/search/cmip6/). Table 2 describes RCM and GCM models selected and used. These climate models were selected based on several criteria, including their ability to accurately simulate precipitation and temperature in the Mediterranean region, as demonstrated in various studies (eg. (Babaousmail et al., 2022)). Furthermore, they were chosen based on their spatial resolution (Bourdeau-Goulet and Hassanzadeh, 2021), their application in several other hydrological studies (Awotwi et al., 2021; Gemechu et al., 2021; Lee et al., 2019; Quansah et al., 2021; Raju and Kumar, 2020) and their performance in research conducted for north African and Mediterranean regions (Brouziyne et al., 2020; Moçayd et al., 2020; Mami et al., 2021; Martínez-Salvador et al., 2021; Moucha et al., 2021; Peres et al., 2020; Saade et al., 2021; Tramblay et al., 2018; Tuel et al., 2021). The CMIP6 global climate models were chosen due to their most recent climate projections, while the EURO-CORDEX regional climate models were selected due to their higher-resolution climate data.

A multi-model ensemble using a simple mean approach was also utilized to deal with the uncertainty induced by different GCMs as indicated by Babaousmail et al. (2022). According to Tebaldi and Knutti (2007), multi-model ensemble average gives more dependable and robust estimates than any individual model. Furthermore, Bourdeau-Goulet and Hassanzadeh (2021) and cited references, have suggested that an ensemble of simulations per climate model is advised to

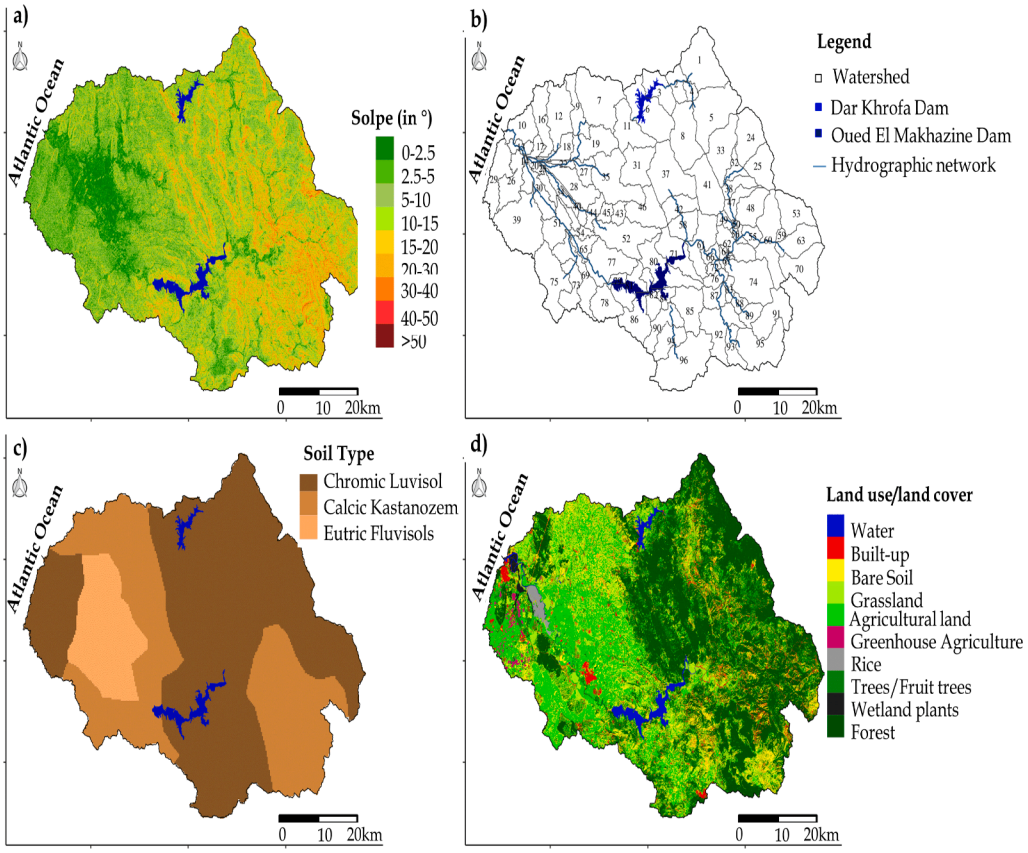

Fig. 4. (a) Slope classes, (b) sub-basins distribution, (c) soil types, and (d) land use/land cover map of Loukkos basin.

represent GCMs "forced response" for CMIP5 and CMIP6. In this present study, we considered three future periods: near (2021–2040), mid (2041–2070), and far (2071–2100) futures. RCPs 4.5 and 8.5 for EURO-CORDEX models and SSPs 2–4.5 and 5–8.5 for CMIP6 models have been considered. It should be noted that the end-of-century forcing of 4.5 and 8.5 W/m^2 is consistent across both the SSPs and RCPs used in this research. Nonetheless, considerable differences persist between SSP 5–8.5 and RCP 8.5. The former assumes approximately 20% higher CO_2 emissions throughout the 21st century. Moreover, SSP 2–4.5 applies a higher starting point for CO_2 emissions than RCP 4.5 but ultimately results in lower emissions with a more gradual decline by the end of the century (Bourdeau-Goulet and Hassanzadeh, 2021). Detailed information of RCPs and SSPs scenarios can be found in (O'Neill et al., 2017; van Vuuren et al., 2011).

In addition, GCMs and also RCMs climate projections often have considerable biases due to systematic model errors such as discretization and spatial averaging within grid cells (Martínez-Salvador et al., 2021; Teutschbein and Seibert, 2012). When climate change effects are incorporated, such as in hydrological effect studies, similar biases may be increased. Therefore, bias correction of GCMs/RCM data is recommended (Awotwi et al., 2021; Brouziyne et al., 2020; Lee et al., 2019; Luo et al., 2018; Teutschbein and Seibert, 2012). In this study, future precipitation and temperature were bias-corrected using the distribution mapping method of the CMhyd (Climate Model data for hydrologic modeling) tool (Rathjens et al., 2016). This non-parametric empirical method corrects the distribution function of simulated climate data using a Gamma transfer function based on the probability distribution of observed values. It was chosen because of its proven effectiveness in precipitation data analysis (Lee et al., 2019; Teutschbein and Seibert, 2012) and its application in various climate settings in previous hydrological studies (Awotwi et al., 2021; Fang et al., 2015; Gemechu et al., 2021; Lee et al., 2019). More details and advantages of this method have been described in (Fang et al., 2015; Teutschbein and Seibert, 2012).

Fig. 3 illustrates the average monthly variation in observed and simulated precipitation, as well as minimum and maximum temperatures, using RCM (1981–2005) and GCM (1981–2014) models. It was concluded that Aladin63, RACMO22E and WRF381P show almost identical patterns with a slight difference in March (16 mm, with relative difference of 30.7%) and December (-14 mm, with relative difference of −11.6%). Earth3Veg and IPSLCM6A also appear to be similar to precipitation observed, especially between April (-0.4%) and November (-5.3%). For minimum temperature, although there is a general agreement in annual amplitudes between simulations and observations, there are some differences in monthly amplitudes (from −0.79 (-5.1%: Jun-Ensemble mean GCMs) to 1.00 °C (6.7%: Octobre-Aladin63 and HIRHAM5). Additionally, for maximum temperature, we notice that the difference is more noticeable than that of minimum temperature. The simulated maximum temperature difference ranging from −4.7 to 8.8 °C, respectively in November with RACMO22E and WRF381P and in January with RACMO22E.

Based on mean changes in annual and seasonal precipitation, minimum and maximum temperatures, as shown in Fig. A.12, it was concluded that almost all models show a decrease in precipitation (with change from −79.8% to 20.7%), which is more pronounced under RCP 8.5/SSP5-8.5 than RCP 4.5/SSP2-4.5. Overall, annual and seasonal precipitation decreases in 2071–2100 are greater than in 2021–2040 and 2041–2071. These results are in agreement with previous studies (Moçayd et al., 2020; El Khalki et al., 2021; Tuel et al., 2021) over Morocco. It can be seen that summer precipitation will change substantially more than winter precipitation, and the spring decline will be more pronounced than the winter decline. Mostly, all models predict a considerable increase in minimum and maximum temperatures, both annually and seasonally, except in summer for HIRHAM5 and RCA4.

Nevertheless, under all scenarios, the strongest increase is expected in 2071–2100 by reaching 7.9 °C (SON-IPSLCM6A) and 8.4 °C (MAM-GFDLESM4) respectively for minimum and maximum temperatures. However, it is crucial to remember that these projections may contain uncertainties and that the egregious values obtained should be interpreted with caution for future use.

Spatial data

a. DEM data:

A digital Elevation Model (DEM) of the Shuttle Radar Topography Mission (SRTM) with 30 m resolution was obtained from Earth Explorer portal (https:/earthexplorer.usgs.gov) of the United States Geological Survey (USGS). In order to generate a DEM raster, four images were mosaicked, reprojected into the WGS84/UTM Zone 30 system, and lastly clipping to Loukkos basin. Each pixel in this DEM raster provides a precise altitude value ranging from 0 to 1,677 m. Subsequently, this DEM was used to delineate the watershed, generate elevation, and calculate the watershed slope. The DEM and slope of Loukkos basin are illustrated in Figs. 1-b and 4-a, -a, respectively.

b. Soil data:

Soil data (1:50000) utilized in this study is the Harmonized world soil database v1.2 (YYYY), which was obtained from the United Nations' Food and Agriculture Organization. Furthermore, data based on soil qualities, including texture, soil water content, hydrological soil group, soil depth, bulk density, and organic carbon content, was adjusted to the needed format. Soil codes were adapted and incorporated into the SWAT 2012 database. The soil types were classified into three classes (Fig. 4-c). The Chromic Luvisol are the most dominant soils dominant soils in Loukkos basin. They occupy 58.0% of the basin total area followed by 32.2% for Calcic Kastanozem, and 9.8% for Eutric Fluvisols.

c. Land use/land cover:

Land use/Land cover information was generated using a Random forest (RF) (Breiman, 2001) supervised classification, based on Sentinel-2 satellite data for 2020, to generate the following land cover classes: water, built-up, bare soil, grassland, agricultural land, greenhouse agriculture, rice, trees and fruit trees, wetland plants, and forest. We note that image correction and classification steps used in this study were performed following the methodology of Acharki (2022). 36 Sentinel-2 images used were downloaded via Copernicus Open Access Hub (Copernicus, 2021) provided by European Space Agency (ESA) based on their availability and cloud absence. Then, a pre-processing step was applied to eliminate atmospheric effects. Used images were also mosaiced and projected from WGS84/UTM Zone 29 (EPSG: 32629) projection system to WGS84/UTM Zone 30 (EPSG: 32630) system. For image classification, ground truth data were randomly and manually selected. They were based on field knowledge, photos taken during field trip inventory and completed by high resolution satellite images from Google Earth (Acharki et al., 2020; Acharki et al., 2022). Therefore, 2,563 training samples for ground truth data were generated. These ground truth data were randomly partitioned into two parts: The initialization of RF classification model was assigned to 70% of the dataset, while the 30% remaining was used for model validation and performance evaluation. At polygon level, the allocation was done to have an independent set of pixels between training and validation steps. In order to assess classification accuracy, kappa coefficient was used and overall accuracy was determined using a confusion matrix, which is a widely used approach for determining classification accuracy (Foody, 2002). The software QGIS (QGIS Development Team, 2021), Orfeo ToolBox (OTB) (OTB, 2018) and R language programming (R Core Team, 2020) were used. The overall accuracy was 98.4%, with a kappa index of 0.98, thus indicating that classification LULC was more accurate. The most frequent land use in Loukkos basin is forest, which covers about 29.8% of the total area, followed by trees/fruit trees and agricultural land that cover comparable areas (Fig. 4-d).

SWAT model

Model setup and simulation

The Soil Water Assessment Tool (SWAT) developed by Arnold et al. (1998), is a continuous, spatially, daily time-step and semi-distributed hydrological model (Abbaspour, 2015; Arnold et al., 1998; Neitsch et al., 2011). It was originally designed to assess the impact of climate and land management practices on watershed hydrology in large, complex watersheds over extended periods (Arnold et al., 1998). Although being developed and calibrated in a distinct climatic zone, the model has been successfully utilized in various regions around the world, including the Mediterranean (Martínez-Salvador et al., 2021; Taia et al., 2023; Echogdali et al., 2022; Erraioui et al., 2023; Saade et al., 2021). In addition, extensive testing and calibration have been conducted to ensure the model's reliability in predicting water stress and vegetation response under various conditions. Previous research has applied SWAT to assess the implications of climate change scenarios and examine adaptive management practices to mitigate climate change-induced impacts (Martínez-Salvador et al., 2021; Saade et al., 2021; Gemechu et al., 2021). Nevertheless, it is critical to consider that the model's accuracy and ability to simulate future scenarios are contingent on the availability and input data quality, such as climate projections, land management practices, and assumptions concerning how hydrological processes may respond to climate change. SWAT simulates various parameters such as streamflow, sediment loss transport, and nutrient flow on a watershed scale. Besides, each watershed is separated into sub-basins, which are further subdivided into Hydrologic Response Units (HRUs), thus allowing a high level of spatial detail simulation. The SWAT model includes various components, such as hydrology, weather conditions and land management, which are described in detail by Neitsch et al. (2011). The water balance equation below (Neitsch et al., 2011) is used to simulate streamflow in SWAT.

$$SW_t = SW_o + \sum_{i=1}^{t} (R_{day} - Q_{surf} - ET_a - W_{seep} - Q_{gw})_i \quad (1)$$

where SW_t is the final soil water content at time t, SW_o is initial soil water content, R_{day} is daily precipitation, Q_{surf} is surface runoff, ET_a is daily actual evapotranspiration, W_{seep} is percolation amount and Q_{gw} is daily amount of return flow. All variables are expressed in mm/day. SWAT output can be saved in different time steps (daily, monthly, or yearly), although basic water balance runs on a daily time step. In this study, a monthly time step was evaluated. To estimate evapotranspiration three methods are offered in SWAT: Hargreaves (Hargreaves and Samani, 1985), Priestley-Taylor (Priestley and Taylor, 1972), and Penman–Monteith (Monteith, 1965). Hargreaves method was selected in this study due to its recommendation by the FAO when observed meteorological data are unavailable and its application in previous Moroccan watersheds (Brouziyne et al., 2020; Choukri et al., 2020; Erraioui et al., 2021; Taia et al., 2021; Tramblay et al., 2018; Taia et al., 2023).

Subsequently, the Loukkos basin was divided into 94 sub-basins following watershed delineation step (Fig. 4-b). A total of 1200 HRUs were created by combining slope classes (Fig. 4 soil map (Fig. 4 and a land use/land cover map (Fig. 4-d).

Sensitivity analysis, calibration and validation

SWAT model's simulation capabilities were evaluated through calibration, validation, sensitivity, and uncertainty analysis, which was conducted using SWAT-CUP (Calibration Uncertainties Program) software with the SUFI-2 (Sequential Uncertainty Fitting Version 2) algorithm (Abbaspour, 2015). SUFI-2 was chosen because of its robustness in achieving optimization and quantifying the uncertainty (Mehan et al., 2019; Taia et al., 2021), and has been used in previous studies that have simulated hydrological responses (Gemechu et al., 2021; Choto and Fetene, 2019; López-Ballesteros et al., 2020; Mehan et al., 2019; Bal

Table 4
Sensitive parameter calibration and fitted values for Loukkos basin.

Parameter	Description	p-value	t-stat	Fitted value	Rank
r_CN2.mgt	SCS runoff curve number II	0.00	19.68	11.24	1
r_SOL_AWC().sol	Available water capacity (mm H_2O mm $soil^{-1}$)	0.00	−5.02	0.012	2
v_ESCO.hru	Soil evaporation compensation factor	0.012	2.612	49.45	3
v_GW REVAP.gw	Groundwater "revap" coefficient	0.02	−2.45	0.02	4
v_GWQMN.gw	Threshold depth of water in the shallow aquifer required for return flow to occur (mm H_2O)	0.04	−2.09	874.46	5
v_CH N2.rte	Manning's "n" value for the main channel	0.16	−1.40	3.94	6
v_OV N.hru	Manning's "n" value for overland flow	0.267	−1.12	−0.43	7
v_REVAPMN.gw	Threshold depth of water in the shallow aquifer for "revap" to occur (mm H_2O)	0.28	1.08	−0.35	8
v_CH K2.rte	Effective hydraulic conductivity in main channel alluvium (mm h^{-1})	0.69	0.39	0.96	9
r_HRU SLP.hru	Average slope steepness (mm^{-1})	0.89	0.14	0.16	10

Note: "v_" and "r_" mean a replacement, and a relative change to the initial parameter values, respectively. Rank is based on p-value and t-stat Abbaspour (2011).

et al., 2021). Sensitivity analysis is crucial to reduce parameters number that needs to be changed in SWAT (Abbaspour, 2015; Martínez-Salvador et al., 2021). In this research, the sensitivity analysis was carried out on the most commonly modified parameters in literature during streamflow calibration Arnold et al. (2012). Thus, ten parameters were chosen for the model calibration (see Table 4). The curve number (CN2) and soil available water capacity (SOL_AWC) are the most influential parameters followed by soil evaporation coefficient (ESCO) and underground-related parameters (GW REVAP and GWQMN). SWAT model was calibrated from 1981–1997, with an initial three-year warm-up period. This warm-up period allows the model to run efficiently, and simulation results from this time period were not included in the analysis. It was further validated from 1997–2015, except for St. Dar khorfa and St. Sidi Ayad Soussi where observed streamflow was unavailable after 2003 and 2013, respectively.

To calibrate the model at each hydrological station, the parameters associated to the upstream sub-basins of each hydrological station were altered individually. Then, before moving on to the next station, optimal parameters were validated and their values were set. This was done by varying only parameters in intermediate sub-basins. This approach, in comparison to single calibration, increases the parameter freedom degree (Erraioui et al., 2021), although it takes more time and requires more simulations. Thus, each station undergoes three to five iterations of 600 simulations for calibration and one iteration of 600 simulations for validation. The following statistical metrics were used to assess the model's performance: Nash–Sutcliffe efficiency (NSE) coefficient (Nash and Sutcliffe, 1970), and percent bias (PBIAS) (Gupta et al., 1999). The NSE coefficient refers to the simulation's correlation with observations and is widely used to evaluate the prediction performance of hydrologic models (Quansah et al., 2021; Gemechu et al., 2021). When NSE value is greater than 0.36, the model calibration results are regarded as "acceptable", and when it is greater than 0.75, it is considered "very good" (Moriasi et al., 2007). The PBIAS measures the average tendency of simulated data to differ from their recorded counterparts. When PBIAS's absolute value is less than 25%, it indicates satisfactory simulation performance (Moriasi et al., 2007). It is important to note that calibrating the SWAT model to the current situation in the Loukkos basin (as in other regions) does not necessarily guarantee accurate predictions of future conditions with increased irrigation and severe water stress. This is due to the potential for future changes in climate, land use, water management practices, and population growth to significantly alter the basin's hydrological processes, which may not be accounted for in the calibrated model. As a result, inaccuracies in model projections are conceivable.

Furthermore, any investigation with a calibrated model must include an uncertainty analysis in the result (Abbaspour et al., 2007). Therefore, it is necessary to implement uncertainty analysis to gain more confidence in numerical modeling. In SUFI2, uncertainty in parameters, expressed as ranges (uniform distributions), accounts for all sources of uncertainties such as uncertainty in driving variables (precipitation or temperature), conceptualization of model, parameters, or measured streamflow. Propagation of uncertainties in the parameters leads to uncertainty in model outputs, which are expressed as the 95% probability distributions (Abbaspour, 2015). Thus, the fit quantification between simulated and observed, expressed in 95PPU, can be performed using two statistical indices: p-factor and r-factor. The p-factor is the proportion of observed data associated by 95% prediction uncertainty (95PPU) and is estimated using Latin hypercube sampling at 2.5% and 97.5% levels of output variable's cumulative distribution. Simultaneously, the r-factor indicates relative thickness of 95PPU band. According to Abbaspour (2015), good calibration results for discharge simulation should be >0.70 for p-factor and around 1 for r-factor, while in a low-quality data it may be sufficient to consider a p-factor above 0.5.

$$r-factor = \frac{\frac{1}{n}\sum_{t_i=1}^{n}\left(Y^{M}_{t_i,97.5\%} - Y^{M}_{t_i,2.5\%}\right)}{\sigma_{obs}} \quad (2)$$

$$NSE = 1 - \frac{\sum_{i=1}^{n}(O_i - P_i)^2}{\sum_{i=1}^{n}(O_i - O_{avg})^2} \quad (3)$$

$$PBIAS = \frac{\sum_{i=1}^{n}(O_i - P_i)100}{\sum_{i=1}^{n} O_i} \quad (4)$$

where, n is the total number of observations or simulations. i is the number of values. $Y^{M}_{t_i,97.5\%}$ and $Y^{M}_{t_i,2.5\%}$ are the upper and lower boundaries of the 95PPU. σ_{obs} is the standard deviation of the observed streamflow data. O_i is observed streamflow values. P_i is simulated streamflow values. O_{avg} is average observed streamflow. P_{avg} is average simulated streamflow.

Observed and simulated streamflow hydrographs, as well as statistical performance of calibration and validation are summarized in Figs. A.13 and A.14. The quantitative assessment of model efficiency indicates good simulation (NSE >0.77 and PBIAS within ± 10%) on a monthly basis. Furthermore, according to the criteria of Abbaspour (2015), the 95PPU correctly predicted >70% of monthly data for most stations, demonstrating that the calibrated monthly streamflow model accurately recreated monthly streamflow in Loukkos basin.

Results and discussion

Historical streamflow analysis

To assess climate models' capacity to reproduce historical streamflow regimes, the 11 climate models (RCMs and GCMs) were forced as inputs to SWAT calibrated model.

Performance of models

The correlation between observed streamflow and historical

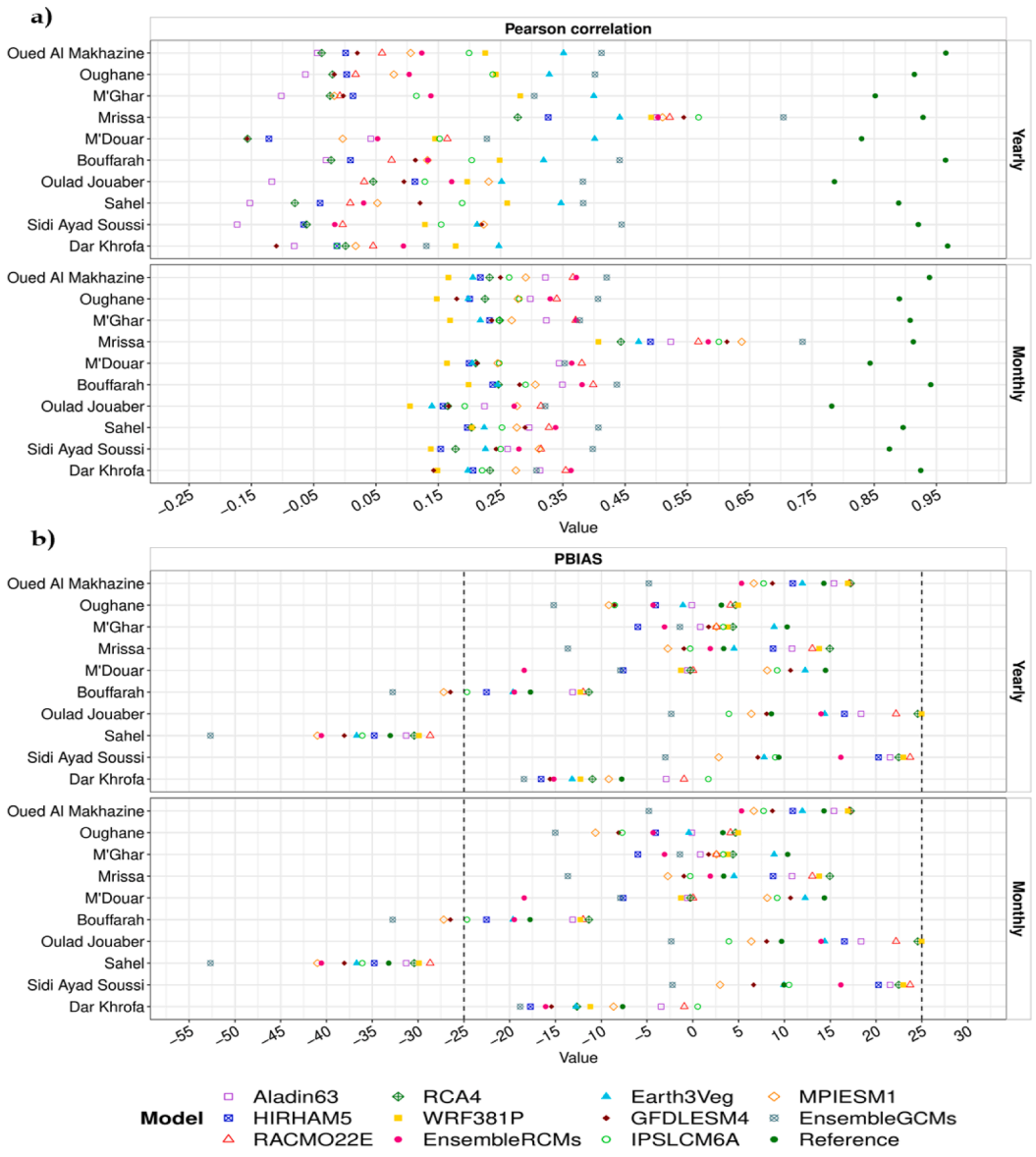

Fig. 5. Statistical parameters (Pearson correlation (a) and PBIAS coefficient (b)) to evaluate streamflow provided from RCM/GCM models (Historical period 1981–2005/1981–2014) and measured data (Reference) at different hydrological stations. The colored symbols represent the eleven RCM/GCM models and the reference data for each station. The sub-panel titles indicate the statistical parameters used for monthly and annual calculations, specifically the Pearson correlation and PBIAS coefficient. Note that the dashed lines between −25 and 25 signify satisfactory simulation performance.

streamflow provided from RCM/GCM models, shown in Fig. 5-a, indicates that the best correlations were found on a monthly basis. Whereas, on an annual basis, negative correlations between −0.01 and −0.17 for Aladin63, HIRHAM5, and RC4 were reported. Overall, EnsembleGCMs presented better correlations. The findings also imply that individual RCM models have a lower correlation than the GCMs model. The upgraded version of CMIP6 could be linked to GCMs' improved performance (Ayugi et al., 2021; Kamruzzaman et al., 2021; Zhu et al., 2021). It can also be noticed that the highest correlations (reaching 0.73) appeared in Mrissa station, which is located in the basin's downstream part and typically receives greater streamflow owing to the contribution of various upstream areas. Upstream stations, on the other hand, may have a lower correlation due to the influence of local factors like topography, land use, and soil conditions. Furthermore, PBIAS findings indicated good results (low PBIAS values) for the majority of stations, indicating that the model is accurately simulating the observed data (Fig. 5-b). Except for Sahel station, where most models significantly underestimate observed streamflow (<−29). This underestimation is also noticeable in reference simulations based on observed climatic data. These findings suggest that uncertainties are more related to model calibration rather than climate models. Therefore, enhancing model calibration may lead to more accurate streamflow predictions. In comparison to other models, EnsembleGCMs, EnsembleRCMs, and GFDLESM4 significantly underestimate streamflow. Despite being the best correlated with the reference model, the ensemble means GCMs/RCMs could not reduce bias compared to individual models. This contrasts previous studies, which indicated that ensemble models reduced bias and uncertainty in predicting streamflow (Giménez et al., 2018; Maharjan et al., 2021). It is worth noting that this issue can be solved by employing another averaging multi-model ensemble approach, such as weighting.

Weighted multi-model averaging, which assigns different weights to each model based on its ability to represent the observed climate, can provide a more accurate representation of climate projections. Besides, several studies (e.g, (Hong et al., 2022)) have shown that weighted multi-model ensembles have potential and can lead to more reliable climate projections and better-informed decision-making. Therefore, we recommend that this approach be used in future research as an alternative to the simple averaging approach.

Streamflow's regime variations

Variations in the streamflow regime were depicted using flow

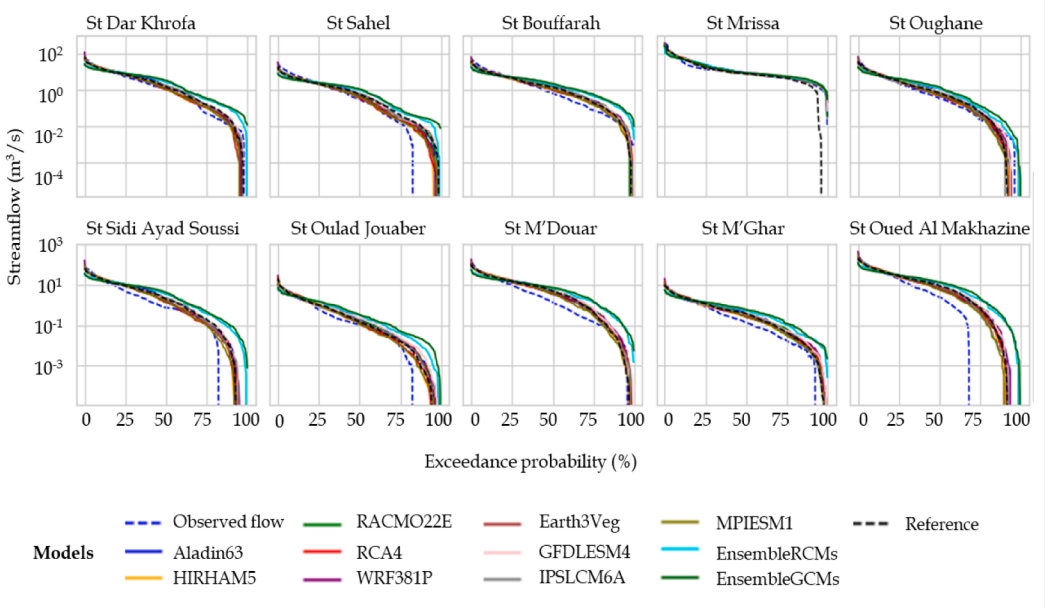

Fig. 6. Exceedance probabilities of the monthly observed streamflow and historical climate models at different hydrological stations.

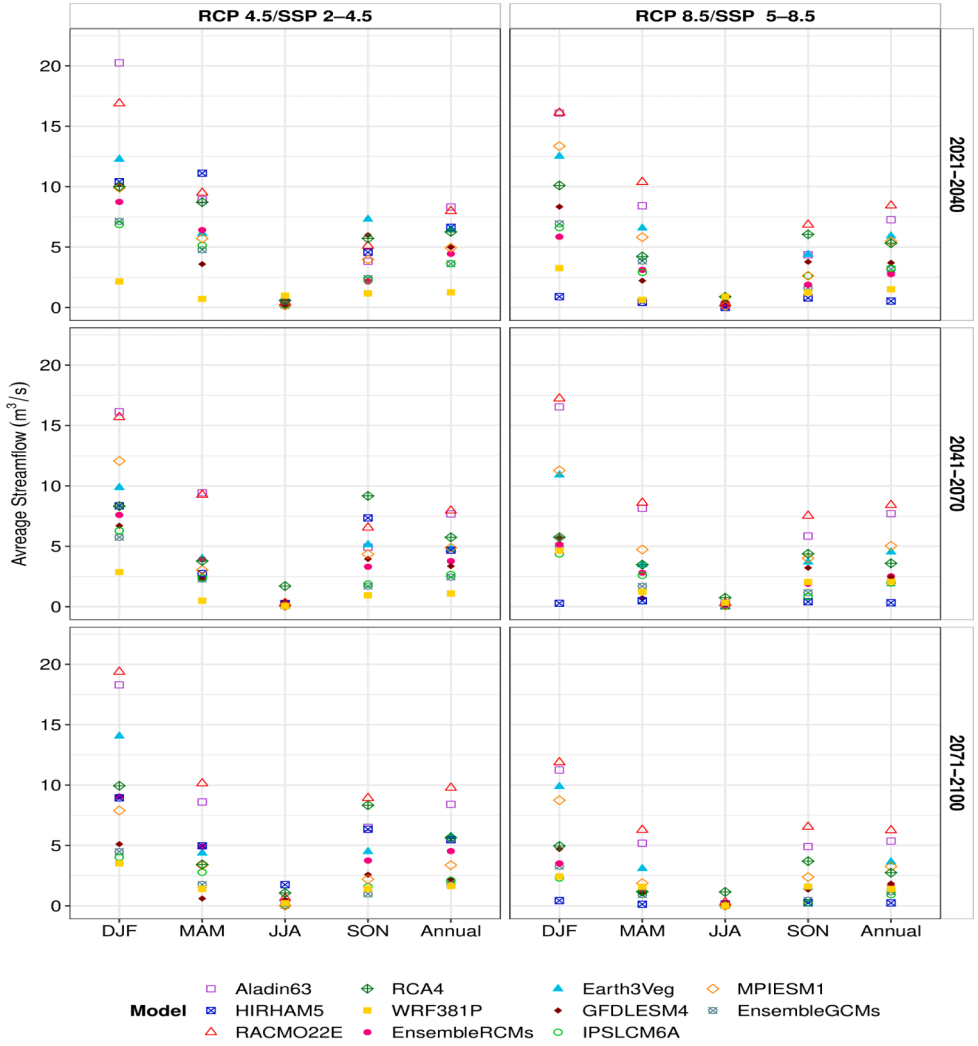

Fig. 7. Avreage annual and seasonal streamflow for 2021–2040, 2041–2070, and 2071–2100 for different RCM and GCM models.

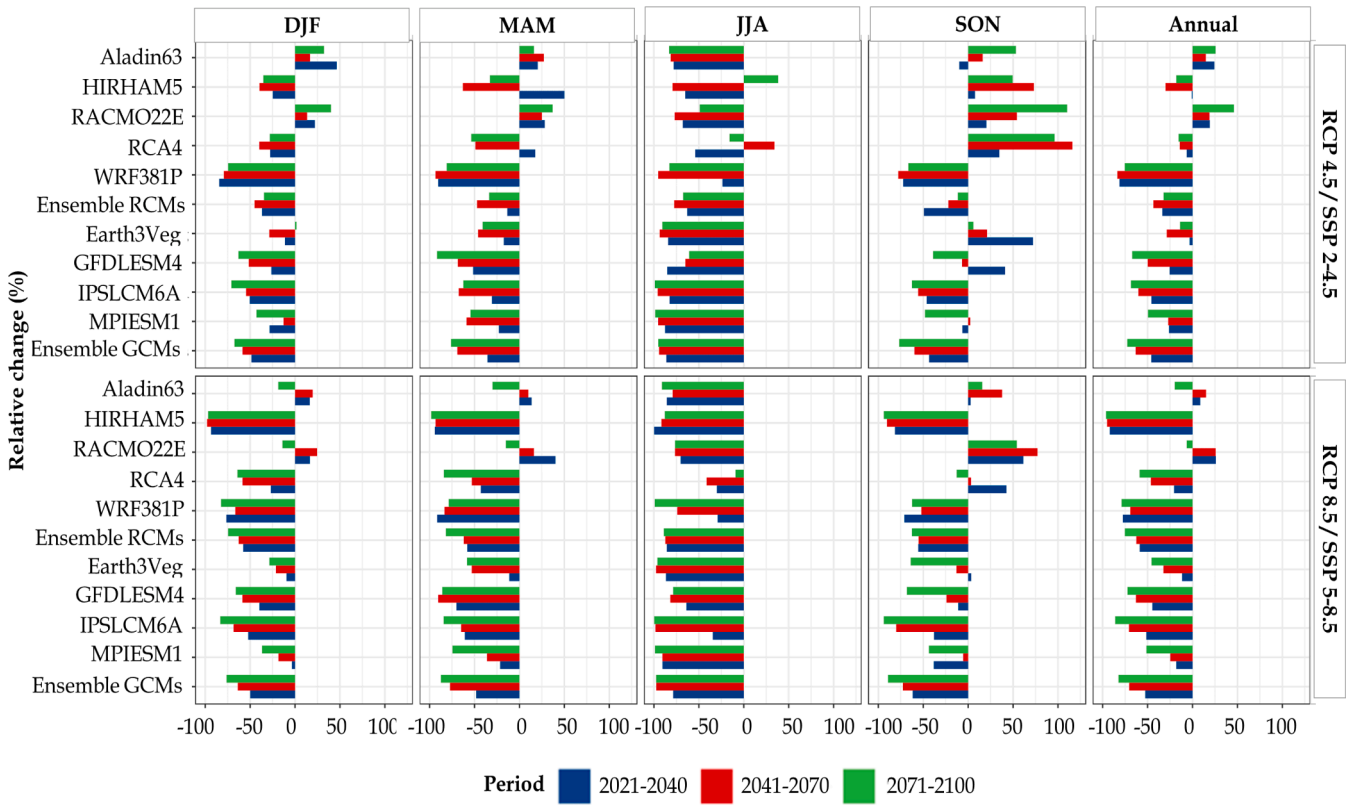

Fig. 8. Temporal relative change in mean annual streamflow for Loukkos basin.

duration curves and log10 normal probability to highlight the visibility of low values in climate model data. The flow duration curves in Fig. 6 reveal that almost all RCM and GCM models overestimate medium and low values, whereas these models underestimate high values. However, extreme streamflows predicted from models tend to be slightly lower than those reported at all stations. These significant underestimations are predominantly observed in EnsembleGCMs and EnsembleRCMs and they could be linked to the multi-model ensemble approach used in this research, which utilizes a single mean method.

Furthermore, the multi-model ensemble's mean is found to be substantially biased, mainly for medium and low values, with a significant overestimation of their exceedance probabilities. It could also be seen from Fig. 6 that individual RCM/GCM models adjust streamflow exceedances rather effectively, except for low flows, where they significantly overestimate the flow with a probability greater than 0.75. The accurately recreating challenge of the low streamflow component is a problem that all models face. As suggested by Fang et al. (2015), this might be a systematic problem with the calibrated hydrologic model.

Climate change impacts on streamflow

Pojected annual and seasonal average streamflow

Fig. 7 summarizes the simulated mean annual and seasonal streamflow of each climate model (RCMs and GCMs) over three periods (near, mid and far futures) and under RCP 4.5/SSP2-4.5 and RCP 8.5/SSP5-8.5 scenarios. Under RCP 4.5/SSP2-4.5, the projected mean annual streamflow is expected to range from 1.1 m^3/s to 9.8 m^3/s during the period 2021–2100. These projections are slightly higher than the overall estimates for the RCP 8.5/SSP5-8.5 scenario, which indicate a streamflow range of 0.2 m^3/s to 8.43 m^3/s. This is in agreement with precipitation disparities between the two scenarios. A yearly comparison also reveals that RCAMO22E produces the highest streamflow values, followed by Aladin63. WRF381P and HIRHAM5, however, obtained the lowest values under RCP 4.5/SSP2-4.5 and RCP 8.5/SSP5-8.5, respectively. Furthermore, it can be seen that, across all models, there is a general trend of higher streamflow during winter (DJF) and lower streamflow during summer (JJA), reflecting the average seasonal precipitation distribution.

Overall, Fig. 7 shows the potential variability and uncertainty in streamflow projections under different climate scenarios and among different models. Which could lead to different outcomes depending on which model is used. Since each climate model has its own strengths and weaknesses, as well as unique climate scenarios, it is not surprising to obtain varying streamflow projections. Thus, it is important to consider a range of potential outcomes and formulate contingency plans for each scenario, especially when making decisions related to water management, infrastructure planning, and other climate-sensitive sectors. Nonetheless, the ensemble mean RCMs and ensemble mean GCMs tend to produce similar outcomes in most cases, indicating that the ensemble means can help mitigate the effects of model uncertainty and provide more reliable projections.

Relative spatio-temporal change in average annual and seasonal streamflow

a. Relative temporal change

Relative changes in annual and seasonal streamflow for all models across three periods and under two scenarios are presented in Fig. 8. It reveals that mean annual basin streamflow is projected to decrease in the future by 82% of models, with a lesser decline in 2021–2040 and a higher reduction in 2071–2100 under RCP 4.5/SSP2-4.5 and RCP 8.5/SSP5-8.5 scenarios. According to the findings, climate change is expected to have significant implications for streamflow regimes in the Loukkos Basin. In general, the anticipated annual streamflow changes are within −81.3% to 24.3% (-92.1% to 26.1%) in 2021–2040, −83.7% to 18.8% (-95.2% to 25.8%) in 2041–2070, and −75.4% to 46.1% (-96.3% to −6.5%) in 2071–2100, respectively under RCP 4.5/SSP2-4.5 (RCP 8.5/SSP5-8.5). Interestingly, for 2021–2040 and under RCP 4.5/SSP2-4.5, MPIESM1 and GFDLESM4 show a moderate decrease in annual streamflow (<30%), while RCA4, Earth3Veg, and HIRHAM5

Table 3
Previous studies about climate change impacts on water resources in Mediterranean region.

Reference	Streamgaging period	Water resources Change (%)
(Choukri et al., 2020)	1980–2010	Water availability: −9.9 to −33.3
(Moçayd et al., 2020)	1971–2017	Runoff: −20.0 to −60.0
(López-Ballesteros et al., 2020)	1980–1999	Streamflow: −20.0
(Mami et al., 2021)	1981–2010	Surface flow: −20.0 to −48.0
		River discharge: −42.0 to −54.0
(Marchane et al., 2017)	1989–2009	Surface runoff: −19.0 to −63.0
(Martínez-Salvador et al., 2021)	1993–2018	Streamflow: −46.3 to −52.4
	2003–2018	and −46.6 to −55.8
(Milewski et al., 2019)	1979–2007	Runoff: 13.8
(Saade et al., 2021)	2003–2015	−23 to −45
(Tramblay et al., 2013)	1984–2010	Surface runoff: −30 to −57
(El Khalki et al., 2021)	1985–2014	Runoff: −57.4 to −86.6
(Acharki, 2020)	-	Surface water: −0.75 to −33.65
(Candela et al., 2016)	1984–2008	Runoff: −49.5
(Driouech, 2010)	1956–2000	−20.0 to −30.0

depict a slight annual streamflow decline (<10%). WRF381P, in contrast, demonstrated a significant annual streamflow reduction (>60%). On the other hand, RACMO22E and Aladin63 revealed a considerable increase in annual streamflow. This predicted increment might be explained by an increase in annual precipitation, particularly during winter (DJF). It is notable that, for 2070–2100 and under RCP 8.5/SSP5-8.5, annual streamflow decreased slightly and moderately in RACMO22E and Aladin63, respectively. Moreover, Earth3Veg, MPIESM1, and RCA4 exhibited a high decline in annual streamflow (<60%), whereas GFDLESM4, WRF381P, IPSLCM6A, and HIRHAM5 showed a significant yearly streamflow decline (>60%). Overall future periods, ensemble mean RCMs indicate reductions by 32.3% (58.8%), whereas ensemble mean GCMs reveal declines by 45.9% (52.6%) under RCP 4.5/SSP2-4.5 (RCP 8.5/SSP5-8.5). Similar results were reported by El Khalki et al. (2021), who concluded that, using five RCMs and GR2M models, discharge of Oued El Abid basin will decrease sharply from 57.4 to 86.6 in 2031–2060 and 2061–2090. Moreover, Moçayd et al. (2020) and Tramblay et al. (2013) found largely similar results, indicating that under RCP P4.5 and RCP 8.5, the average annual streamflow will significantly decrease from 20% to 60% and from 30% to 57% in Makhazine dam catchment and Loukkos basin, respectively.

However, our annual relative changes are slightly higher than those found in other Mediterranean watersheds, particularly in Aracthos River basin-Greece (almost −20%) (López-Ballesteros et al., 2020), El Kalb River-Lebanon (-23% to −45%) (Saade et al., 2021), and Tafna watershed-Algeria (-20% to −48%) (Mami et al., 2021). As indicated in the results, different emission scenarios resulted in a wide range of

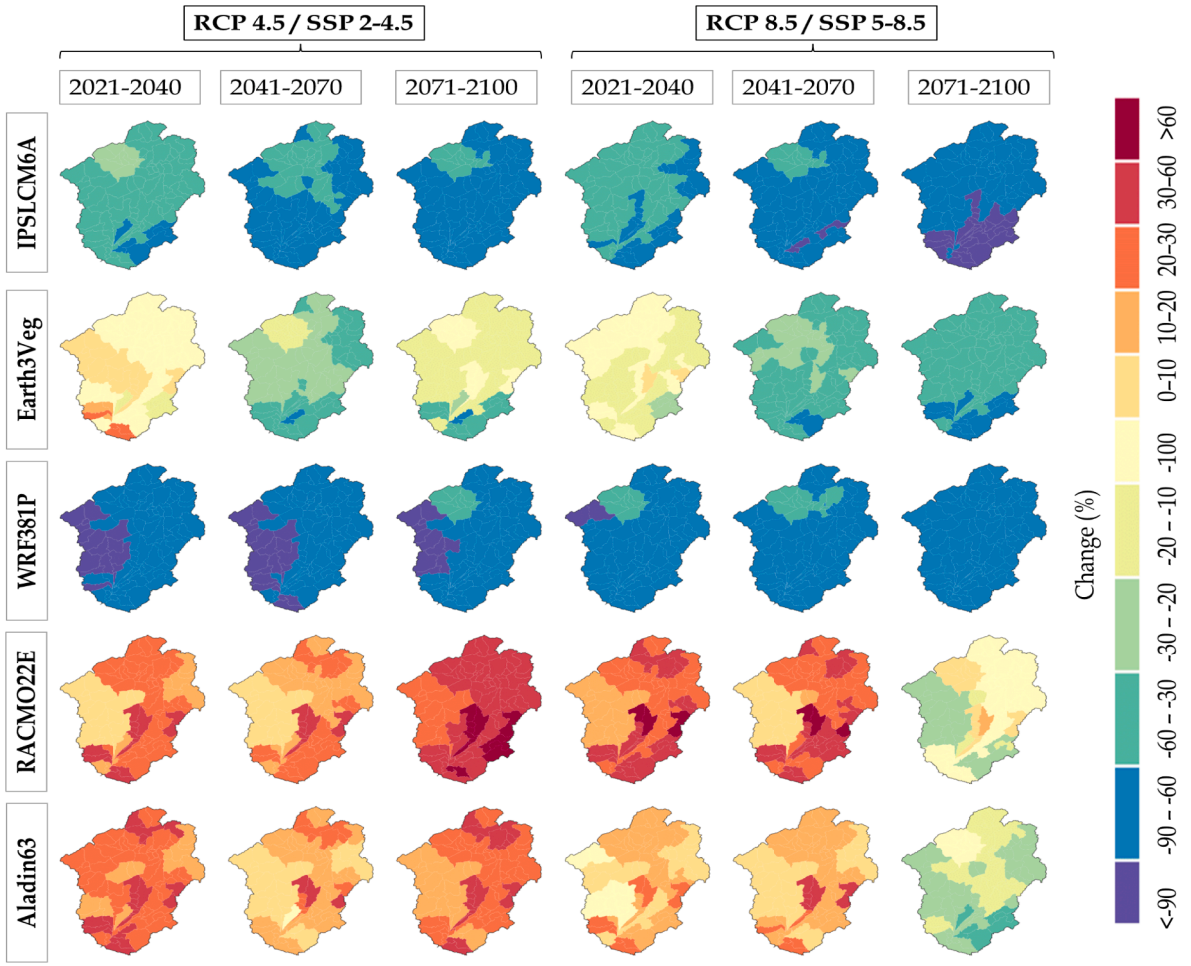

Fig. 9. Spatial relative change in mean annual streamflow in 2021–2040, 2041–2070, and 2071–2100 under RCP 4.5/SSP2-4.5 and RCP 8.5/SSP5-8.5 scenarios as compared to 1981–2020.

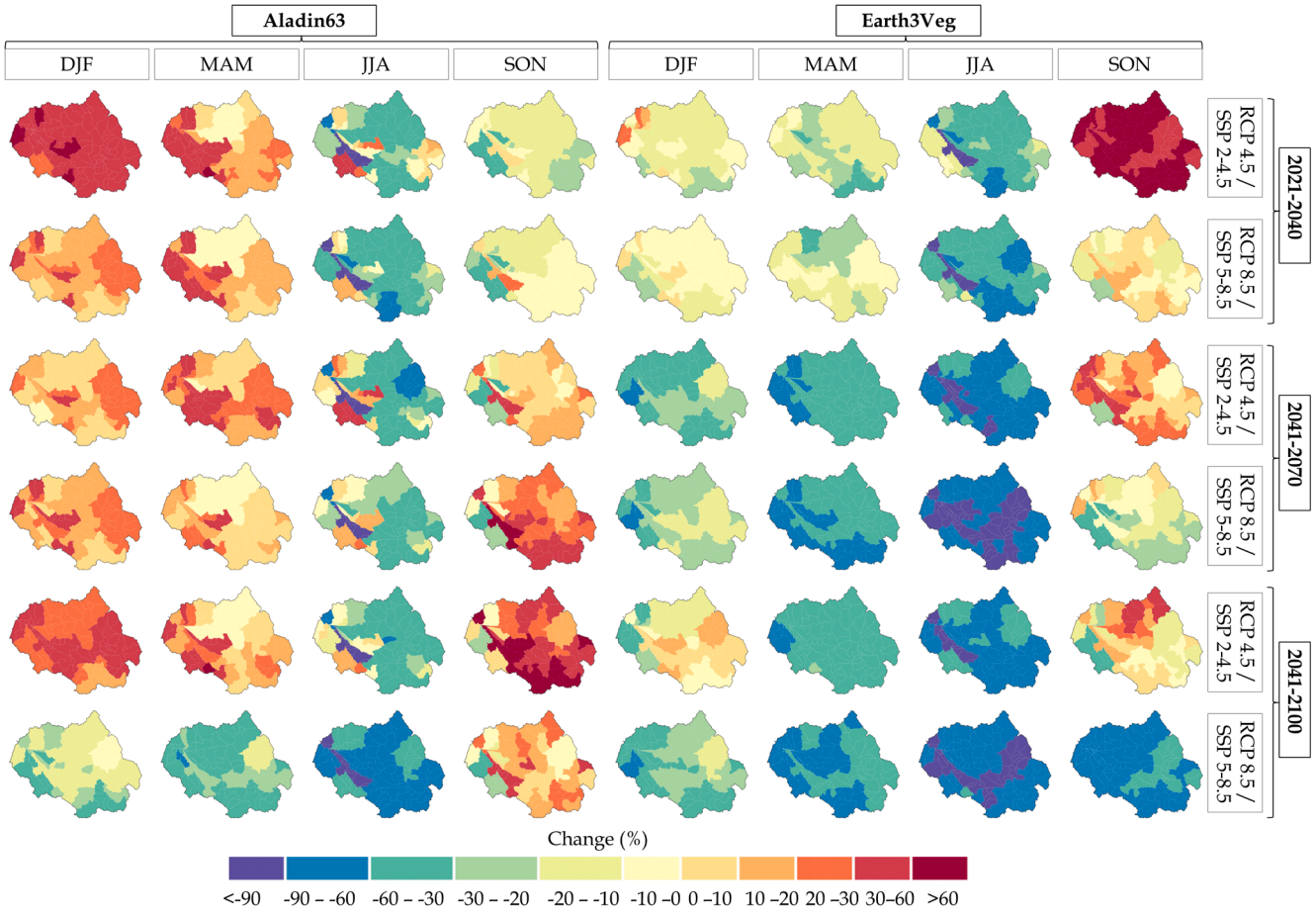

Fig. 10. Spatial relative change in seasonal streamflow in three periods for Aladin63 and Earth3Veg under RCP 4.5/SSP2-4.5 and RCP 8.5/SSP5-8.5 scenarios.

future projections. It can be observed in Fig. 8 that for all models, the projected changes indicate a more pronounced decrease/increase under RCP 8.5/SSP5-8.5 than under RCP4.5/SSP2-4.5. This is consistent with previous studies (El Khalki et al., 2021; Moçayd et al., 2020; Martínez-Salvador et al., 2021; Nilawar and Waikar, 2019; López-Ballesteros et al., 2020; Saade et al., 2021; Tramblay et al., 2013), which are illustrated in Table 3. This difference between scenarios could be because RCP 8.5/SSP5-8.5 is a very high baseline scenario without mitigation. In contrast, RCP 4.5/SSP2-4.5 is an intermediate emission stabilization scenario with mitigation.

Similarly to annual, the future mean seasonal streamflow is projected to decrease in all seasons except autumn (SON). Among the models, 55% and 27% indicate an increase under RCP 4.5/SSP2-4.5 and RCP 8.5/SSP5-8.5 scenarios, respectively. For instance, the projected changes in autumn streamflow range from −93.9% (IPSLCM6A/2071–2100) to 116.0% (RCA4/2041–2070) among different models. While some models show a decline, others exhibit an upward trend. However, it should be noted that such changes in streamflow have the potential to cause droughts or flooding events.

From Fig. 8, it is concluded that the decrease in mean seasonal streamflow is most during summer (JJA) and will reach −99.8% (HIRHAM5/2021–2040 and IPSLCM6A/2071–2100). These summer streamflow reductions may seem large in percentage, but they are actually a departure from very small baseflow values. These findings are in line with those of a previous study (López-Ballesteros et al., 2020), which found that the greatest reductions in streamflow occur in summer, followed by autumn. They also indicated that the decline will be less noticeable in winter and spring. In contrast, the study of El Khalki et al. (2021) revealed that the relative change reduces in winter and spring. It should be highlighted that even minor reductions in streamflow during other seasons can have significant implications for water availability and management in water-stressed regions. Hence, sustainable water management strategies need to consider the magnitude and timing of projected streamflow changes. For Ensemble mean RCMs (Ensemble mean GCMs), average spring streamflow is expected to decrease by 58.0% (48.1%), 62.0% (77.2%), and 81.8% (87.4%) under RCP 8.5/SSP5-8.5 scenario for near, mid, and far futures, respectively. As expected, when compared to RCP 8.5/SSP5-8.5, these shifts are clearly less negative under RCP 4.5/SSP2-4.5, with differences ranging from −48.1% (Ensemble mean RCMs-2071–2100) to −8.2% (Ensemble mean GCMs-2041–2070). Overall season, the magnitude of reduction is greater in RCP 8.5/SSP5-8.5 scenario than in RCP 4.5/SSP2-4.5 scenario.

In anticipation of the significant reduction in streamflow that is likely to occur by the end of this century, Morocco is implementing various measures. These include constructing 50 new dams by 2050 with the aim of increasing storage capacity to 32 billion m^3 and promoting water efficiency by modernizing irrigation systems. The adoption of innovative techniques like precision agriculture, remote sensing, and artificial intelligence is also expected to enhance irrigation efficiency and water management. Nonetheless, further research is required to understand the role of dams in water management and their potential impact on future irrigation practices, particularly in light of the challenges posed by climate change.

b. Relative spatial change

Projected relative spatial change in annual and seasonal streamflow at different periods and scenarios are provided in Figs. 9 and 10, respectively. From Fig. 9, it can be seen that relative future change in

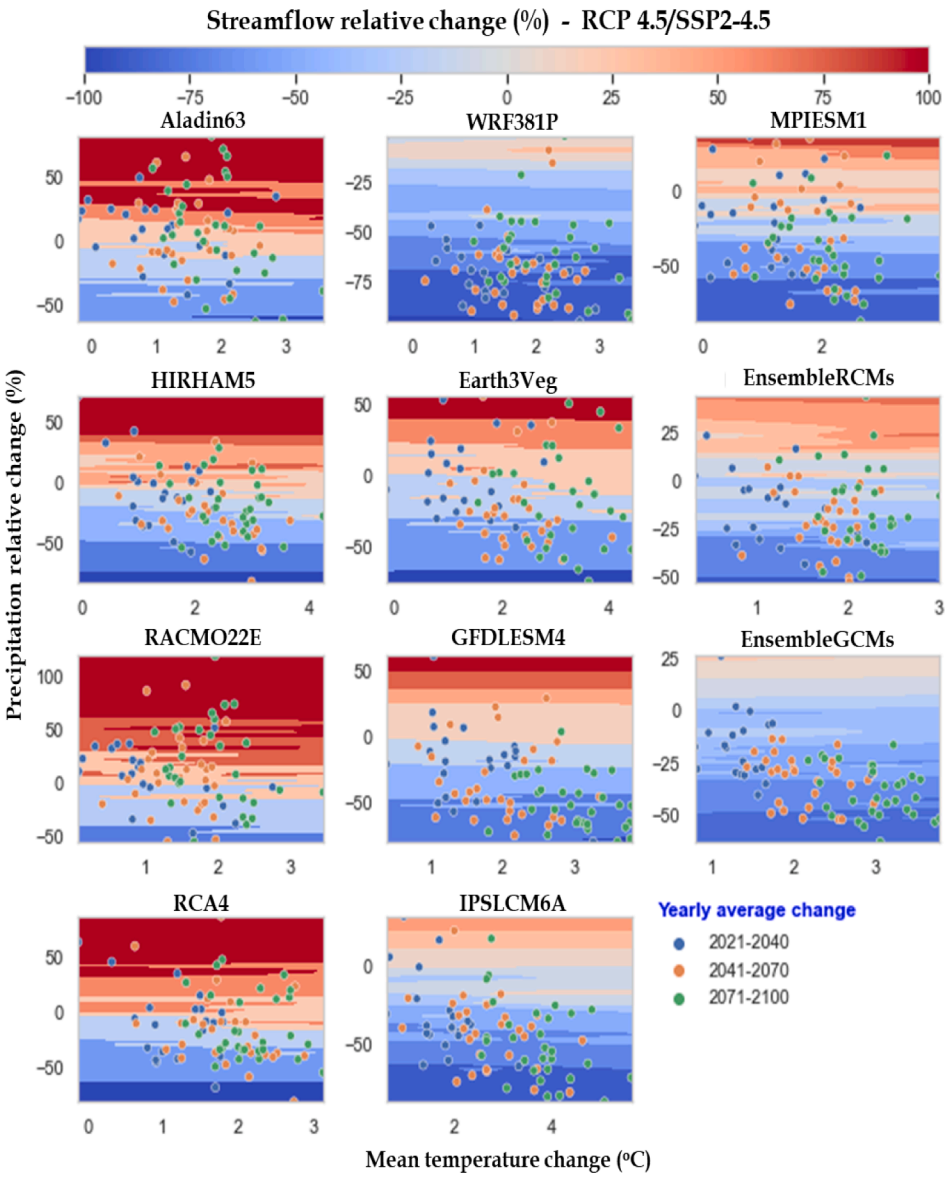

Fig. 11. Annual streamflow responses to changes in precipitation and temperature, relative to baseline period (1981–2014), over Loukkos basin for different RCM and GCM models under RCP 4.5/SSP2-4.5 scenario.

annual streamflow differs by RCM and GCM models.

Aladin63 and RACMO22E indicate annual streamflow gains with relative changes ranging between 0%-60% in almost all periods and scenarios. This information can aid decision-makers in making informed choices regarding water allocation, storage infrastructure, and irrigation practices. However, these gains are expected to decrease from 2021–2040 to 2041–2070 and then increase from 2041–2070 to 2071–2100, highlighting the need for long-term planning. Decision-makers can use this information to anticipate future changes in water availability and make proactive decisions. When compared to Aladin63, RACMO22E displays more positive variations. Furthermore, central, northwest, and south sub-basins are the most affected by these gains. This information can help decision-makers prioritize water management efforts in these regions. Conversely, under the RCP 8.5 scenario during 2071–2100, annual streamflows would be mostly dropping in most basins, with a 30% decline in the southwest. In contrast, WRF381P's annual streamflow shift differed considerably from the other two RCM models, indicating a large reduction of −60% to −90% across most of basin. The projections also reveal that the largest reductions (<-90%) are more likely to occur in the basin's northern part, where the Dar Khrofa dam is located, notably under RCP 4.5 scenario. This information is critical for decision-makers responsible for water management in the Loukkos basin as they can prioritize their efforts in the northern region to protect the Dar Khrofa dam. Building additional water storage facilities, such as reservoirs, can help mitigate the impact of reduced streamflow during dry periods. They may also consider implementing measures to increase water efficiency, such as reducing water losses in distribution systems or promoting water-saving technologies, to ensure the long-term sustainability of the Loukkos basin's water resources. Although Earth3Veg predicted some increases in streamflow, particularly for 2021–2040 under SSP2-4.5 scenario and more frequently for western and northern sub-basins, annual streamflow declines over the other periods in most sub-basins. For example, southwestern sub-basins are projected to see the most declines (-60% to −90%), notably in 2071–2100. These sub-basins are renowned for their agricultural land, and the projected decrease in streamflow could have severe consequences. To address these potential impacts, decision-makers need to take action by implementing measures such as promoting the use of efficient irrigation technologies, supporting drought-resistant crop cultivation, and encouraging farmers to adopt sustainable water

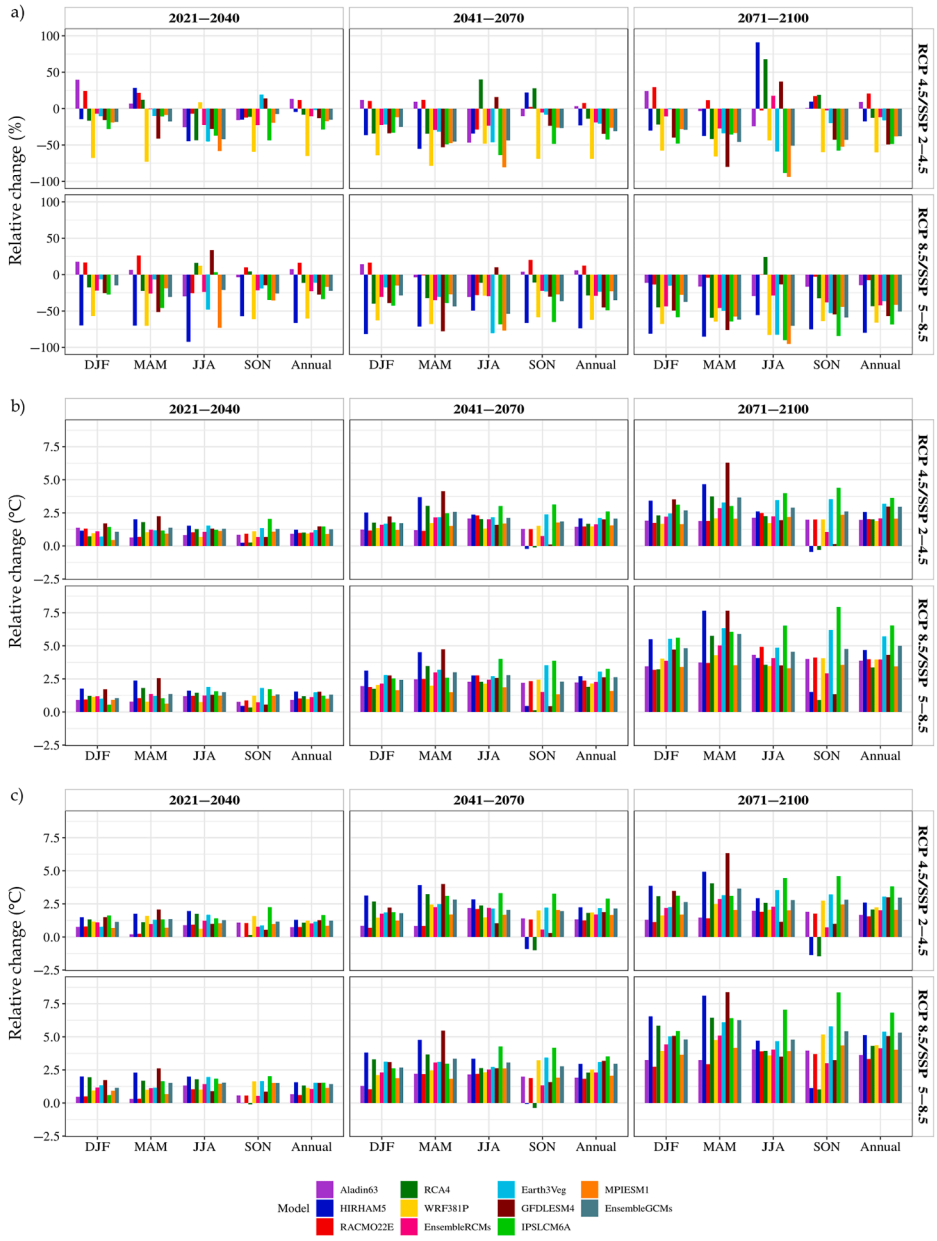

Fig. A.12. Annual and seasonal variations in precipitation, minimum and maximum temperatures for different RCM and GCM models RCP 4.5/SSP2-4.5 and RCP 8.5/SSP5-8.5 scenarios.

management practices. For IPSLCM6A, the annual streamflow will be substantially reduced in both scenarios, following a southwest-northeast gradient. We estimate that these losses would increase from 2021–2040 to 2071–2100, and are more significant in the northwest and southwest sub-basins, particularly under SSP5-8.5, which represents a variation of more than −90%.

We note that, for Fig. 10, we chose to focus on one RCM model (ALADIN63) and one GCM model (EC-Earth3-veg) as they offered the most consistent and reliable projections of streamflow changes across the range of climate scenarios and time periods considered. By presenting results from these two models, we aim to provide a clear and concise picture of potential streamflow changes in the Loukkos watershed under different climate scenarios, without overwhelming readers with a large number of models to consider.

On the other hand, future seasonal streamflow variation fluctuates widely depending on the season, period, climate model and scenario, and is anticipated to drop by 2071–2100, as illustrated in Fig. 10. Aladin63 indicates an overall increasing shift in winter and spring streamflow for most of Loukkos basins, with a few exceptions, such as the north and center sub-basins, where negative changes were found in spring. Summer streamflow reveals a mixed change, with most sub-basins likely to follow a decrease, while the northwest and southwest sub-basins, are likely to project an increment, except in 2071–2100 under RCP 8.5. Similarly, there is a mixed change in autumn streamflow. With a few exceptions, it appears to be declining in 2021–2040, while rising in 2041–2070 and 2071–2100 in most sub-basins. In summary, Aladin63's spatial distributions of seasonal streamflow change differ from Earth3Veg's. Overall, Earth3Veg model shows a general drop over most sub-basins between winter and summer and a substantial increase in autumn under both scenarios, with a few exceptions. From Fig. 10, it can be observed that more negative spatial variation is expected in summer than in winter and spring.

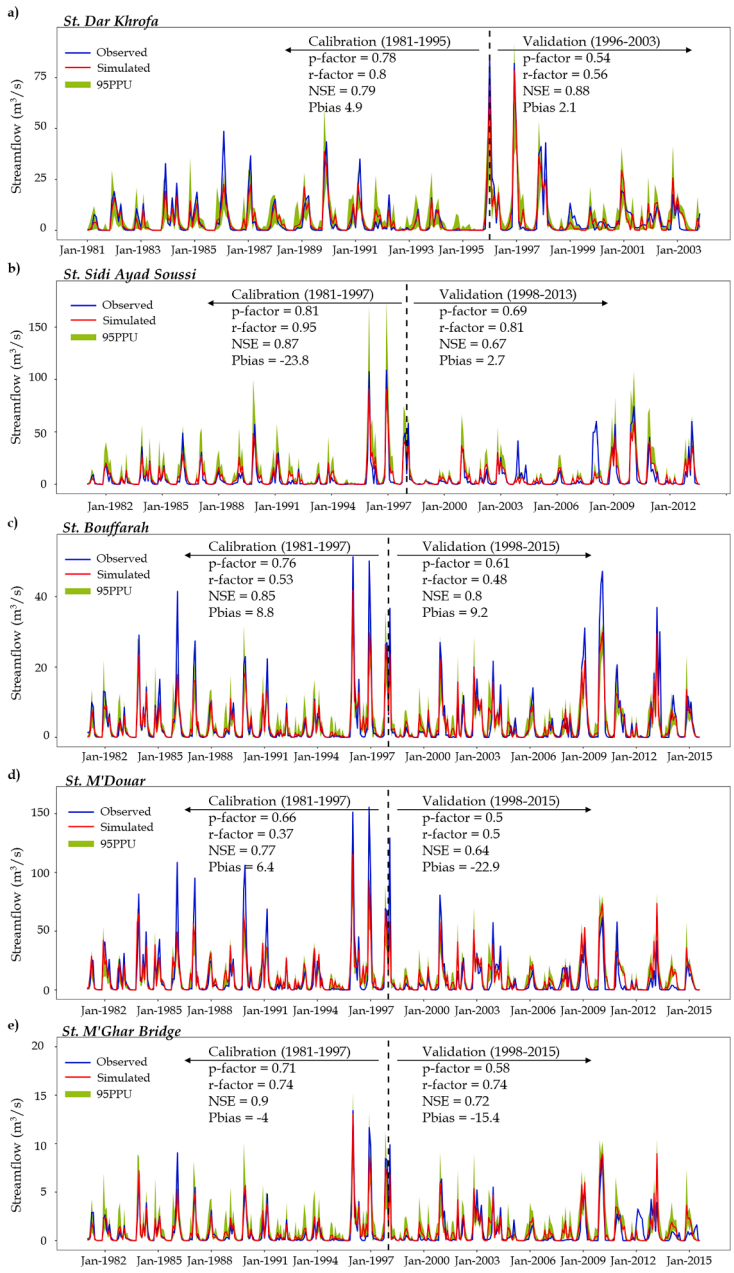

Fig. A.13. Comparison of monthly observed and simulated streamflow during calibration and validation at different gauging stations, on Loukkos basin.

Sensitivity of streamflow to precipitation and temperature changes

Streamflow change responses to future precipitation and temperature change are presented in Figs. 11 and A.15. Overall, changes in streamflow are primarily influenced by changes in precipitation. Similar findings have been reported by Ndhlovu and Woyessa (2021) and Yin et al. (2018). Temperature variations, on the other hand, appear to have little impact on streamflow. Fig. 11 shows also that Aladin63, RACMO22E, RCA4, and HIRHAM5 models predict the most significant changes.

The WRF381P and IPSLCM6A models anticipated mainly negative changes in streamflow due to their underestimation of projected precipitation relative to the reference period. More negative precipitation and warmer temperatures are predicted under RCP 8.5/SSP5-8.5 scenario (Fig. A.15), resulting in negative changes in streamflow. Compared to RCM models, the GCM models predicted only minor increases in streamflow. This indicates that the RCM models anticipate a positive change in flow rates. This could be explained by precipitation drop magnitude derived from ensemble means GCMs compared to ensemble means RCMs under both scenarios.

Conclusion

Climate services are crucial in providing decision-makers with the information they need to implement successful policies and strategies for climate change adaptation and water resource management. In this study, we investigated climate change impacts on future streamflow using SWAT model, for the first time, in Loukkos basin (northwestern Morocco). To set up SWAT model's input data, five regional climate models (EURO-CORDEX), four global climate models (CMIP6), and their ensemble mean were bias-corrected using distribution mapping. Medium and high representative concentration pathways (RCPs and SSPs) were considered for near (2021–2040), mid (2041–2070), and far (2071–2100) futures and compared to baseline period 1981–2020. In addition, land use/land cover map was generated using Random Forest

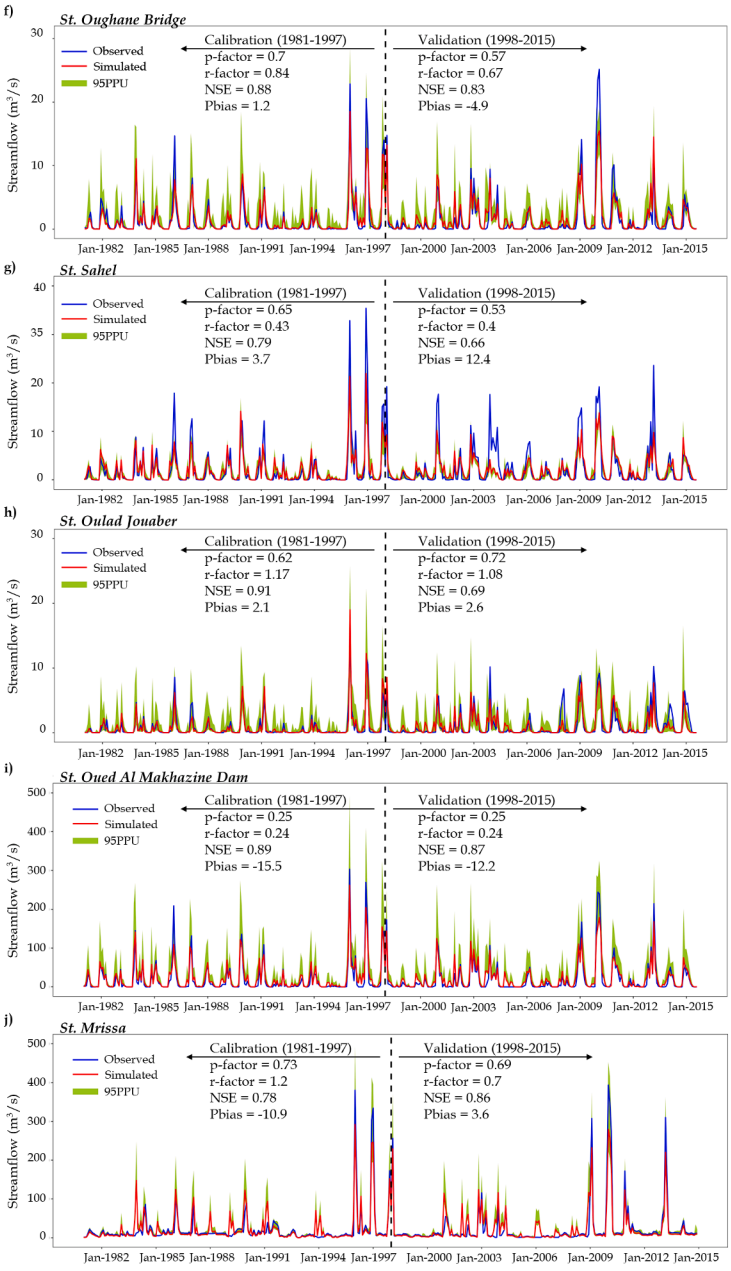

Fig. A.14. Comparison of monthly observed and simulated streamflow during calibration and validation at different gauging stations, on Loukkos basin. (continued).

algorithm. Using SUFI-2 algorithm in SWAT-CUP, SWAT model was further calibrated and validated at ten hydrological stations. The main conclusions are summarized as follows:

(1) SWAT model's calibration and validation revealed good performance (NSE >0.77 and PBIAS within ±10%) in streamflow simulations on a monthly basis.
(2) When compared to individual models (GCMs/RCMs), using a simple mean approach for multi-ensemble models may not result in a significant reduction in bias. This emphasizes the significance of thoroughly selecting appropriate models to achieve accurate predictions. Therefore, it may be more beneficial for future research to use a weighted multi-ensemble approach that takes into account the performance of individual models.
(3) For most models, there was an increase in the annual minimum and maximum temperatures, with an increment of 0.9–6.5 °C and 0.6–6.8 °C, respectively. In addition, climate change will also have an impact on precipitation. Overall, annual precipitation is expected to drop from 79.8% to 1.9%, while it is expected to rise from 3.4% to 20.7% for some RCM models such as Aladin63 and RACMO22E.
(4) For most models, there was an increase in the annual minimum and maximum temperatures, with an increment of 0.9–6.5 °C and 0.6–6.8 °C, respectively. In addition, climate change will have also an (4) Based on correlation analyses, changes in precipitation have a greater impact on streamflow response compared to increases in air temperature. Besides, the uncertainties in streamflow modeling at some stations, such as Sahel, may be more related to the model calibration rather than the climate models themselves. Nonetheless, further research is needed to improve understanding and to confirm these findings, and

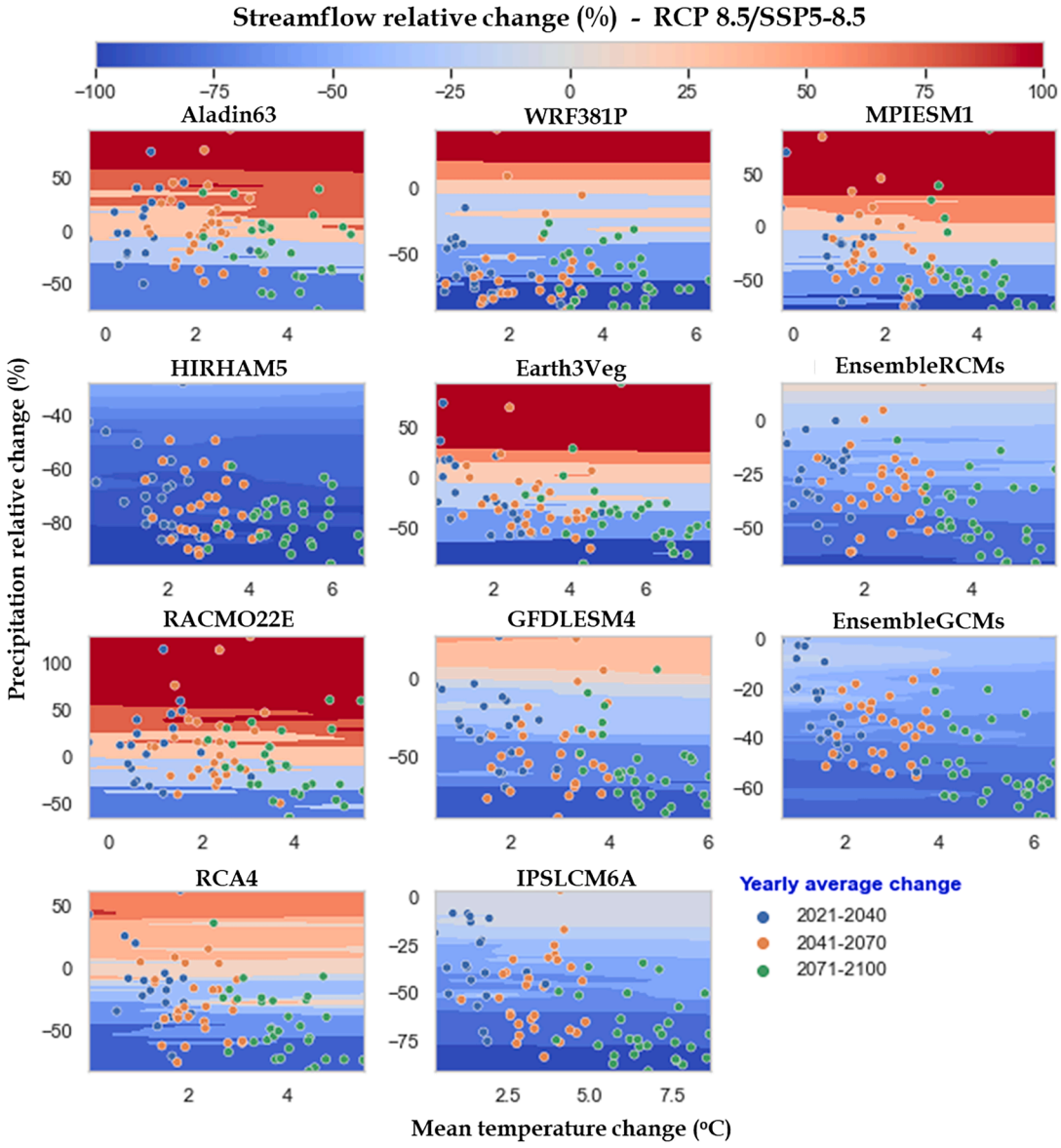

Fig. A.15. Annual streamflow responses to changes in precipitation and temperature, relative to baseline period (1981–2014), over Loukkos basin for different RCM and GCM models under RCP 8.5/SSP5-8.5 scenario.

explore the factors that affect streamflow response and uncertainties in more detail.

(5) Projected streamflow indicates a rise or decrease, depending on the RCM/GCM model. For instance, 82% of models showed a reduction in annual streamflow. Under RCP 8.5/SSP5-8.5, the magnitude of change varied between −92.1% to 26.1% and −96.3% to −6.5% in 2021–2040 and 2071–2100, respectively. This thus indicates that the change is expected to be gradually aggravated in the far-future (2071–2100). Moreover, seasonal streamflow obviously varies from one model to another depending on the season, future period, and scenario. With this information, decision-makers can prioritize water management efforts and plan for the long-term sustainability of water resources in the Loukkos basin. They can take proactive measures such as constructing additional water storage facilities, promoting the use of water-efficient technologies, supporting drought-resistant crop cultivation, and adopting sustainable water management practices to ensure the availability of water resources in the future.

Therefore, the study's findings underscore the importance of climate services, as policymakers need to consider projected changes in streamflow and precipitation patterns to develop sustainable water resource management policies and adaptation measures in the Loukkos basin, particularly in irrigated areas. In summary, the study's methodology and findings can also be extended to other regions facing similar challenges, demonstrating the value of climate services in informing decision-making and policy development at both the local and global scales. Climate services, through harnessing cutting-edge climate research and technology, can help society adapt to climate change's impacts and build resilience for a sustainable future. Ultimately, further investigations on other hydrological process components and their future evolution are suggested.

CRediT authorship contribution statement

Siham Acharki: Conceptualization, Methodology, Software, Validation, Formal analysis, Visualization, Data curation, Writing - original draft, Writing - review & editing, Supervision. **Soufiane Taia:** Methodology, Investigation, Validation, Writing - review & editing. **Youssef Arjdal:** Investigation, Conceptualization, Writing - review & editing. **Jochen Hack:** Methodology, Writing - review & editing.

Declaration of Competing Interest

The authors declare that they have no known competing financial interests or personal relationships that could have appeared to influence the work reported in this paper.

Data availability

Data will be made available on request.

Acknowledgment

The publication of this article was funded by the Open Access Publishing Fund of Leibniz University Hannover. The authors would like to express their deepest gratitude to Dr. Daniela Jacob (Editor-in-Chief) and the reviewers for their valuable comments on the manuscript. We thank also Abdeslam Acharki for accompanying us on field trips. Thank you to Loukkos Hydraulic Basin Agency and Loukkos Regional Agricultural Development Office for providing us with meteorological and hydrological data-sets. We also acknowledge the Earth System Grid Federation (ESGF) and its sponsors for storing and giving total access to Euro-CORDEX and CMIP6 outputs.

Continued results

Fig. A.12, A.13, A.14, A.15

References

Abbaspour, K., 2011. Swat-Cup2: SWAT Calibration and Uncertainty Programs Manual Version 2. Technical Report. https://doi.org/10.1007/s00402-009-1032-4.

Abbaspour, K., 2015. SWAT – CUP: SWAT Calibration and Uncertainty Programs – A User Manual. Technical Report. https://doi.org/10.1007/s00402-009-1032-4.

Abbaspour, K., Yang, J., Maximov, I., Siber, R., Bogner, K., Mieleitner, J., Zobrist, J., Srinivasan, R., 2007. Modelling hydrology and water quality in the pre-alpine/alpine thur watershed using swat. J. Hydrol. 333, 413–430. https://doi.org/10.1016/j.jhydrol.2006.09.014.

Acharki, S., 2020. Contributions of modeling and remote sensing in climate change impact on water resources study: Application to irrigated areas Loukkos and Gharb (Morocco). Abdelmalek Essaädi University. Ph.D. thesis.

Acharki, S., 2022. Planetscope contributions compared to sentinel-2, and landsat-8 for lulc mapping. Remote Sens. Appl.: Soc. Environ. 27, 100774.

Acharki, S., Amharref, M., Frison, P.L., Bernoussi, A.S., 2020. Crop mapping in Loukkos perimeter (Morocco): Radar and optical remote sensing contributions. French J. Photogramm. Remote Sens. 222, 15–29. 10.52638/rfpt.2020.481.

Acharki, S., El Qorchi, F., Arjdal, Y., Amharref, M., Bernoussi, A.S., Ben Aissa, H., 2022. Soil erosion assessment in Northwestern Morocco. Remote Sens. Appl.: Soc. Environ. 25, 100663 https://doi.org/10.1016/j.rsase.2021.100663.

Aghsaei, H., Dinan, N., Moridi, A., Asadolahi, Z., Delavar, M., Fohrer, N., Wagner, P., 2020. Effects of dynamic land use/land cover change on water resources and sediment yield in the Anzali wetland catchment, Gilan, Iran. Sci. Total Environ. 712, 136449 https://doi.org/10.1016/j.scitotenv.2019.136449.

Arnold, J., Srinivasan, R., Muttiah, R., Williams, J., 1998. Large area hydrologic modeling and assessment part I: model development 1. JAWRA J. Am. Water Resour. Assoc. 34, 73–89.

Arnold, J.G., Bieger, K., White, M.J., Srinivasan, R., Dunbar, J.A., Allen, P.M., 2018. Use of decision tables to simulate management in swat+. Water 10, 713.

Arnold, J.G., Moriasi, D.N., Gassman, P.W.K., Abbaspour, C., White, M.J., Srinivasan, R., Jha, M.K., 2012. Swat: Model use, calibration, and validation. Trans. ASABE 55, 1491–1508. 10.13031/2013.42256.

Awotwi, A., Annor, T., Anornu, G., Quaye-Ballard, J., Agyekum, J., Ampadu, B., Nti, I., Gyampo, M., Boakye, E., 2021. Climate change impact on streamflow in a tropical basin of Ghana, West Africa. J. Hydrol.: Regional Stud. 34, 100805 https://doi.org/10.1016/j.ejrh.2021.100805.

Ayugi, B., Zhihong, J., Zhu, H., Ngoma, H., Babaousmail, H., Rizwan, K., Dike, V., 2021. Comparison of cmip6 and cmip5 models in simulating mean and extreme precipitation over east africa. Int. J. Climatol. 41 https://doi.org/10.1002/joc.7207.

Babaousmail, H., Hou, R., Ayugi, B., Sian, K.T.C.L.K., Ojara, M., Mumo, R., Chehbouni, A., Ongoma, V., 2022. Future changes in mean and extreme precipitation over the mediterranean and sahara regions using bias-corrected cmip6 models. Int. J. Climatol. 42, 7280–7297.

Bal, M., Dandpat, A., Naik, B., 2021. Hydrological modeling with respect to impact of land-use and land-cover change on the runoff dynamics in budhabalanga river basing using arcgis and swat model. Remote Sens. Appl.: Soc. Environ. 23, 100527 https://doi.org/10.1016/j.rsase.2021.100527.

Bieger, K., Arnold, J.G., Rathjens, H., White, M.J., Bosch, D.D., Allen, P.M., Volk, M., Srinivasan, R., 2017. Introduction to swat+, a completely restructured version of the soil and water assessment tool. JAWRA J. Am. Water Resour. Assoc 53, 115–130.

Boucher, O., Denvil, S., Levavasseur, G., Cozic, A., Caubel, A., Foujols, M.A., Meurdesoif, Y., Cadule, P., Devilliers, M., Ghattas, J., Lebas, N., Lurton, T., Mellul, L., Musat, I., Mignot, J., Cheruy, F., 2018. IPSL IPSL-CM6A-LR model output prepared for CMIP6 CMIP historical Earth System Grid Federation. Technical Report, 10.22033/ESGF/CMIP6.5195.

Boucher, O., Servonnat, J., Albright, A., Aumont, O., Balkanski, Y., Bastrikov, V., Bekki, S., Bonnet, R., Bony, S., Bopp, L., Braconnot, P., Brockmann, P., Cadule, P., Caubel, A., Cheruy, F., Codron, F., Cozic, A., Cugnet, D., D'Andrea, F., Davini, P., de Lavergne, C., Denvil, S., Deshayes, J., Devilliers, M., Ducharne, A., Dufresne, J., Dupont, E., Éthé, C., Fairhead, L., Falletti, L., Flavoni, S., Foujols, M., Gardoll, S., Gastineau, G., Ghattas, J., Grandpeix, J., Guenet, B., Guez, L., Guilyardi, E., Guimberteau, M., Hauglustaine, D., Hourdin, F., Idelkadi, A., Joussaume, S., Kageyama, M., Khodri, M., Krinner, G., Lebas, N., Levavasseur, G., Lévy, C., Li, L., Lott, F., Lurton, T., Luyssaert, S., Madec, G., Madeleine, J., Maignan, F., Marchand, M., Marti, O., Mellul, L., Meurdesoif, Y., Mignot, J., Musat, I., Ottlé, C., Peylin, P., Planton, Y., Polcher, J., Rio, C., Rochetin, N., Rousset, C., Sepulchre, P., Sima, A., Swingedouw, D., Thiéblemont, R., Traore, A., Vancoppenolle, M., Vial, J., Vialard, J., Viovy, N., Vuichard, N., 2020. Presentation and Evaluation of the IPSL-CM6A-LR Climate Model. J. Adv. Model. Earth Syst. 12. 10.1029/2019MS002010.

Bouramdane, A.A., 2022. Assessment of cmip6 multi-model projections worldwide: Which regions are getting warmer and are going through a drought in africa and morocco? what changes from cmip5 to cmip6? Sustainability 15, 690.

Bourdeau-Goulet, S., Hassanzadeh, E., 2021. Comparisons Between CMIP5 and CMIP6 Models: Simulations of Climate Indices Influencing Food Security, Infrastructure Resilience, and Human Health in Canada. Earth's Future 9, 1–17. https://doi.org/10.1029/2021EF001995.

Breiman, L., 2001. Machine learning. In: Random Forests. Kluwer Academic Publishers, pp. 5–32. https://doi.org/10.1023/A:101093340.

Brouziyne, Y., Abouabdillah, A., Chehbouni, A., Hanich, L., Bergaoui, K., McDonnell, R., Benaabidate, L., 2020. Assessing hydrological vulnerability to future droughts in a Mediterranean watershed: Combined indices-based and distributed modeling approaches. Water (Switzerland) 12. https://doi.org/10.3390/W12092333.

Brouziyne, Y., Abouabdillah, A., Hirich, A., Bouabid, R., Zaaboul, R., Benaabidate, L., 2018. Modeling sustainable adaptation strategies toward a climate-smart agriculture in a Mediterranean watershed under projected climate change scenarios. Agric. Syst. 162, 154–163. https://doi.org/10.1016/j.agsy.2018.01.024.

Bui, M., Lu, J., Nie, L., 2021. Evaluation of the Climate Forecast System Reanalysis data for hydrological model in the Arctic watershed Målselv. J. Water Climate Change 1–24. https://doi.org/10.2166/wcc.2021.346.

Candela, L., Tamoh, K., Olivares, G., Gómez, M., 2016. Climate and land use changes on streamflow and subsurface recharge in the Fluvià Basin, Spain. Water (Switzerland) 8. https://doi.org/10.3390/w8060228.

Choto, M., Fetene, A., 2019. Impacts of land use/land cover change on stream flow and sediment yield of gojeb watershed, omo-gibe basin, ethiopia. Remote Sens. Appl.: Soc. Environ. 14, 84–99. https://doi.org/10.1016/j.rsase.2019.01.003.

Choukri, F., Raclot, D., Naimi, M., Chikhaoui, M., Nunes, J., Huard, F., Hérivaux, C., Sabir, M., Pépin, Y., 2020. Distinct and combined impacts of climate and land use scenarios on water availability and sediment loads for a water supply reservoir in northern Morocco. Int. Soil Water Conserv. Res. 8, 141–153. https://doi.org/10.1016/j.iswcr.2020.03.003.

Christensen, O., Drews, M., Dethloff, K., Ketelsen, K., Hebestadt, I., Rinke, A., 2007. Technical report 06-17 The HIRHAM Regional Climate Model Version 5 (β)) Jens Hesselbjerg Christensen Danish Climate Centre, DMI Foundation for Polar and Marine Research Colophon. Danish Meteorol. Inst., Copenhagen, Denmark. 5, 1–22.

Copernicus, 2021. Copernicus Open Data Hub. https://scihub.copernicus.eu. available online.

Daniel, M., Lemonsu, A., Déqué, M., Somot, S., Alias, A., Masson, V., 2018. Benefits of explicit urban parameterization in regional climate modeling to study climate and city interactions. Clim. Dyn. 52, 2745–2764. https://doi.org/10.1007/s00382-018-4289-x.

Di Virgilio, G., Ji, F., Tam, E., Nishant, N., Evans, J.P., Thomas, C., Riley, M.L., Beyer, K., Grose, M.R., Narsey, S., et al., 2022. Selecting cmip6 gcms for cordex dynamical downscaling: model performance, independence, and climate change signals. Earth's Future 10.

Donnelly, C., Ernst, K., Arheimer, B., 2018. A comparison of hydrological climate services at different scales by users and scientists. Climate Services 11, 24–35. https://doi.org/10.1016/j.cliser.2018.06.002.

Döscher, R., Acosta, M., Alessandri, A., Anthoni, P., Arneth, A., Arsouze, T., Bergmann, T., Bernadello, R., Bousetta, S., Caron, L., Carver, G., Castrillo, M., Catalano, F., Cvijanovic, I., Davini, P., Dekker, E., Doblas-Reyes, F., Docquier, D., Echevarria, P., Fladrich, U., Fuentes-Franco, R., Gröger, M., v. Hardenberg, J., Hieronymus, J., Karami, M., Keskinen, J.P., Koenigk, T., Makkonen, R., Massonnet, F., Ménégoz, M.,

Miller, P., Moreno-Chamarro, E., Nieradzik, L., van Noije, T., Nolan, P., O'Donnell, D., Ollinaho, P., van den Oord, G., Ortega, P., Prims, O., Ramos, A., Reerink, T., Rousset, C., Ruprich-Robert, Y., Le Sager, P., Schmith, T., Schrödner, R., Serva, F., Sicardi, V., Madsen, S., Smith, B., Tian, T., Tourigny, E., Uotila, P., Vancoppenolle, M., Wang, S., Wårlind, D., Willén, U., Wyser, K., Yang, S., Yepes-Arbós, X., Zhang, Q., 2021. The EC-Earth3 Earth System Model for the Climate Model Intercomparison Project 6. Geoscientific Model Development Discussions, 1–9010.5194/gmd-2020-446.

Driouech, F., 2010. Winter precipitation distribution over Morocco under climate change: downscaling and uncertainties. Toulouse University, France. Ph.D. thesis.

Driouech, F., ElRhaz, K., Moufouma-Okia, W., Arjdal, K., Balhane, S., 2020. Assessing future changes of climate extreme events in the cordex-mena region using regional climate model aladin-climate. Earth Syst. Environ. 4, 477–492.

Dunne, J., Horowitz, L., Adcroft, A., Ginoux, P., Held, I., John, J., Krasting, J., Malyshev, S., Naik, V., Paulot, F., Shevliakova, E., Stock, C., Zadeh, N., Balaji, V., Blanton, C., Dunne, K., Dupuis, C., Durachta, J., Dussin, R., Gauthier, P., Griffies, S., Guo, H., Hallberg, R., Harrison, M., He, J., Hurlin, W., McHugh, C., Menzel, R., Milly, P., Nikonov, S., Paynter, D., Ploshay, J., Radhakrishnan, A., Rand, K., Reichl, B., Robinson, T., Schwarzkopf, D., Sentman, L., Underwood, S., Vahlenkamp, H., Winton, M., Wittenberg, A., Wyman, B., Zeng, Y., Zhao, M., 2020. The GFDL Earth System Model Version 4.1 (GFDL-ESM 4.1): Overall Coupled Model Description and Simulation Characteristics, vol. 12, 10.1029/2019MS002015.

Echogdali, F., Boutaleb, S., Taia, S., Ouchchen, M., Id-Belqas, M., Kpan, R., Abioui, M., Aswathi, J., Sajinkumar, K., 2022. Assessment of soil erosion risk in a semi-arid climate watershed using swat model: case of tata basin, south-east of morocco. Appl. Water Sci. 12, 137.

El Khalki, E., Tramblay, Y., Hanich, L., Marchane, A., Boudhar, A., Hakkani, B., 2021. Climate change impacts on surface water resources in the oued el abid basin, morocco. Hydrol. Sci. J. 10.1080/02626667.2021.1982137.

El Moçayd, N., Kang, S., Eltahir, E., 2020. Climate change impacts on the Water Highway project in Morocco. Hydrol. Earth Syst. Sci. 24, 1467–1483. https://doi.org/10.5194/hess-24-1467-2020.

Erraioui, L., Mafhoum, N., Taia, S., Chao, J., El Mansouri, B., Haida, S., Taj-Eddine, K., 2021. Assessment of the relative impacts of climate changes and anthropogenic forcing on Ouergha watershed hydrology (North-East of Morocco) 234, 1–7. https://doi.org/10.1051/e3sconf/202123400082.

Erraioui, L., Taia, S., Taj-Eddine, K., Chao, J., El Mansouri, B., 2023. Hydrological modelling in the ouergha watershed by soil and water analysis tool. J. Ecolog. Eng. 24, 343–356.

Fan, X., Miao, C., Duan, Q., Shen, C., Wu, Y., 2020. The performance of cmip6 versus cmip5 in simulating temperature extremes over the global land surface. J. Geophys. Res.: Atmospheres 125.

Fang, G.H., Yang, J., Chen, Y.N., Zammit, C., 2015. Comparing bias correction methods in downscaling meteorological variables for a hydrologic impact study in an arid area in China. Hydrol. Earth Syst. Sci. 19, 2547–2559. https://doi.org/10.5194/hess-19-2547-2015.

Filahi, S., Tramblay, Y., Mouhir, L., Diaconescu, E., 2017. Projected changes in temperature and precipitation indices in Morocco from high-resolution regional climate models. Int. J. Climatol. 37, 4846–4863. https://doi.org/10.1002/joc.5127.

Foody, G., 2002. Status of land cover classification accuracy assessment. Remote Sens. Environ. 80, 185–201. https://doi.org/10.1016/S0034-4257(01)00295-4.

Gebrechorkos, S., Bernhofer, C., Hülsmann, S., 2020. Climate change impact assessment on the hydrology of a large river basin in Ethiopia using a local-scale climate modelling approach. Sci. Total Environ. 742, 140504 https://doi.org/10.1016/j.scitotenv.2020.140504.

Gemechu, T.M., Zhao, H., Bao, S., Yangzong, C., Liu, Y., Li, F., Li, H., 2021. Estimation of hydrological components under current and future climate scenarios in guder catchment, upper Abbay Basin, Ethiopia, using the swat. Sustainability (Switzerland) 13. https://doi.org/10.3390/su13179689.

Georgeson, L., Maslin, M., Poessinouw, M., 2017. Global disparity in the supply of commercial weather and climate information services. Sci. Adv. 3 https://doi.org/10.1126/sciadv.1602632.

Giménez, P.O., García-Galiano, S.G., Giraldo-Osorio, J.D., 2018. Improvement of hydroclimatic projections over southeast spain by applying a novel rcm ensemble approach. Water 10. https://doi.org/10.3390/w10010052.

Grose, M.R., Narsey, S., Delage, F., Dowdy, A.J., Bador, M., Boschat, G., Chung, C., Kajtar, J., Rauniyar, S., Freund, M., et al., 2020. Insights from cmip6 for australia's future climate. Earth's. Future 8.

Guo, H., John, J.G., Blanton, C., McHugh, C., Nikonov, S., Radhakrishnan, A., Rand, K., Zadeh, N., Balaji, V., Durachta, J., Dupuis, C., Menzel, R., Robinson, T., Underwood, S., Vahlenkamp, H., Bu, R., 2018. NOAA-GFDL GFDL-CM4 model output prepared for CMIP6 CMIP historical Earth System Grid Federation. Technical Report, 10.22033/ESGF/CMIP6.1402.

Guo, Y., Fang, G., Xu, Y.P., Tian, X., Xie, J., 2020. Identifying how future climate and land use/cover changes impact streamflow in Xinanjiang Basin, East China. Sci. Total Environ. 710, 136275 https://doi.org/10.1016/j.scitotenv.2019.136275.

Gupta, B., Sorooshian, S., Yapo, P., 1999. 9. Status of automatic calibration for hydrologic models: comparison with multilevel expert calibration. J. Hydrol. Eng. 4, 135–143.

Hamed, M.M., Nashwan, M.S., Shiru, M.S., Shahid, S., 2022. Comparison between cmip5 and cmip6 models over mena region using historical simulations and future projections. Sustainability 14.

Hargreaves, G., Samani, Z., 1985. Reference Crop Evapotranspiration From Temperature. Appl. Eng. Agricul. 1, 96–99. 10.13031/2013.26773.

Harmonized world soil database v1.2, FAO SOILS PORTAL — Food and Agriculture Organization of the United Nations.

Hewitt, C.D., Guglielmo, F., Joussaume, S., Bessembinder, J., Christel, I., Doblas-Reyes, J.F., et al., 2021. Recommendations for future research priorities for climate modeling and climate services. Bull. Am. Meteorol. Soc. 102, E578–E588. https://doi.org/10.1175/BAMS-D-20-0103.1.

Hewitt, C.D., Stone, R., 2021. Climate services for managing societal risks and opportunities. Climate Services 23, 100240. https://doi.org/10.1016/j.cliser.2021.100240.

Hong, J., Agustin, W., Yoon, S., Park, J.S., 2022. Changes of extreme precipitation in the philippines, projected from the cmip6 multi-model ensemble. Weather Climate Extremes 37, 100480.

IPCC, 2021. Summary for Policymakers. Climate Change 2021: The Physical Science Basis. Technical Report. Intergovernmental Panel on Climate Change. Available online:https://www.ipcc.ch/report/ar6/wg1/. (accessed on 16 October 2021).

Jose, D., Dwarakish, G., 2020. Uncertainties in predicting impacts of climate change on hydrology in basin scale: a review. Arab. J. Geosci. 13 https://doi.org/10.1007/s12517-020-06071-6.

Kamruzzaman, M., Shahid, S., Islam, A.T., Hwang, S., Cho, J., Zaman, M.A.U., Ahmed, M., Rahman, M.M., Hossain, M.B., 2021. Comparison of cmip6 and cmip5 model performance in simulating historical precipitation and temperature in bangladesh: a preliminary study. Theoret. Appl. Climatol. 145, 1385–1406. https://doi.org/10.1007/s00704-021-03691-0.

Lagrini, K., Ghafiri, A., Ouali, A., Elrhaz, K., Feddoul, R., Elmoutaki, S., 2020. Application of geographical information system (GIS) for the development of climatological air temperature vulnerability maps: An example from Morocco. Meteorol. Appl. 27, 1–17. https://doi.org/10.1002/met.1871.

Larsen, M., Karamitilios, G., Halsnæs, K., She, J., Madsen, K., 2021. Advancing future climate services: Multi-sectorial mapping of the current usage and demand in denmark. Climate Risk Manage. 33, 100335 https://doi.org/10.1016/j.crm.2021.100335.

Lee, M., Im, E., Bae, D., 2019. Impact of the spatial variability of daily precipitation on hydrological projections: A comparison of GCM– and RCM–driven cases in the Han River basin, Korea. Hydrological Processes 2240–2257. https://doi.org/10.1002/hyp.13469.

López-Ballesteros, A., Senent-Aparicio, J., Martínez, C., Pérez-Sánchez, J., 2020. Assessment of future hydrologic alteration due to climate change in the Aracthos River basin (NW Greece). Sci. Total Environ. 733, 139299 https://doi.org/10.1016/j.scitotenv.2020.139299.

Luo, M., Liu, T., Meng, F., Duan, Y., Frankl, A., Bao, A., De Maeyer, P., 2018. Comparing bias correction methods used in downscaling precipitation and temperature from regional climate models: A case study from the Kaidu River Basin in Western China. Water (Switzerland) 10. https://doi.org/10.3390/w10081046.

Maharjan, M., Aryal, A., Talchabhadel, R., Thapa, B.R., 2021. Impact of climate change on the streamflow modulated by changes in precipitation and temperature in the north latitude watershed of nepal. Hydrology 8. https://doi.org/10.3390/hydrology8030117.

Majdi, F., Hosseini, S.A., Karbalaee, A., Kaseri, M., Marjanian, S., 2022. Future projection of precipitation and temperature changes in the middle east and north africa (mena) region based on cmip6. Theoret. Appl. Climatol. 1–14.

Mami, A., Yebdri, D., Sauvage, S., Raimonet, M., Miguel, J., 2021. Spatio-temporal trends of hydrological components: the case of the Tafna basin (northwestern Algeria). J. Water Climate Change. https://doi.org/10.2166/wcc.2021.242.

Marchane, A., Tramblay, Y., Hanich, L., Ruelland, D., Jarlan, L., 2017. Climate change impacts on surface water resources in the Rheraya catchment (High Atlas, Morocco). Hydrol. Sci. J. 62, 979–995. https://doi.org/10.1080/02626667.2017.1283042.

Martínez-Salvador, A., Millares, A., Eekhout, J., Conesa-García, C., 2021. Assessment of streamflow from euro-cordex regional climate simulations in semi-arid catchments using the swat model. Sustainability (Switzerland) 13. https://doi.org/10.3390/su13137120.

Martín-Martín, M., Guerrera, F., Hlila, R., Maaté, A., Maaté, S., Tramontana, M., Serrano, F., Cañaveras, J., Alcalá, F., Paton, D., 2020. Tectono-sedimentary cenozoic evolution of the el habt and ouezzane tectonic units (external rif, morocco). Geosciences 10. https://doi.org/10.3390/geosciences10120487.

Meddi, M., Eslamian, S., 2021. Uncertainties in Rainfall and Water Resources in Maghreb Countries Under Climate Change. Springer International Publishing, pp. 1967–2003, 10.1007/978-3-030-45106-6_114.

Mehan, S., Aggarwal, R., Gitau, M., Flanagan, D.C., Wallace, C., Frankenberger, J., 2019. Assessment of hydrology and nutrient losses in a changing climate in a subsurface-drained watershed. Sci. Total Environ. 688, 1236–1251. https://doi.org/10.1016/j.scitotenv.2019.06.314.

van Meijgaard, E., Ulft, L., Bosveld, F., Lenderink, G., Siebesma, A., 2008. The KNMI regional atmospheric climate model RACMO version 2.1. KNMI number: TR-302.

van Meijgaard, E., van Ulft, L., Lenderink, G., de Roode, S., Wipfler, L., Boers, R., Timmermans, R., 2012. Refinement and application of a regional atmospheric model for climate scenario calculations of Western Europe. Technical Report.

Milewski, A., Seyoum, W., Elkadiri, R., Durham, M., 2019. Multi-Scale Hydrologic Sensitivity to Climatic and Anthropogenic Changes in Northern Morocco. Geosciences 10, 1–22.

Monteiro, L., Sentelhasb, P., Pedraa, G.U., 2018. Assessment of NASA/POWER satellite-based weather system for Brazilian conditions and its impact on sugarcane yield simulation. Int. J. Climatol. 38, 1571–1581.

Monteith, J., 1965. Evaporation and environment. Symposia of the Society for Experimental Biology 205–234.

Moriasi, D.N., Arnold, J.G., Van Liew, M.W., Bingner, R.L., Harmel, R.D., Veith, T.L., 2007. Model Evaluation Guidelines for Systematic Quantification of Accuracy in Watershed Simulations. Trans. ASABE 50, 885–900. https://doi.org/10.1234/590.

Moucha, A., Hanich, L., Tramblay, Y., Saaidi, A., Gascoin, S., Martin, E., Le Page, M., Bouras, E., Szczypta, C., Jarlan, L., 2021. Present and future high-resolution climate forcings over semiarid catchments: Case of the tensift (Morocco). Atmosphere 12, 1–24. https://doi.org/10.3390/atmos12030370.

Müller, W., Jungclaus, J., Mauritsen, T., Baehr, J., Bittner, M., Budich, R., Bunzel, F., Esch, M., Ghosh, R., Haak, H., Ilyina, T., Kleine, T., Kornblueh, L., Li, H., Modali, K., Notz, D., Pohlmann, H., Roeckner, E., Stemmler, I., Tian, F., Marotzke, J., 2018. A Higher-resolution Version of the Max Planck Institute Earth System Model (MPI-ESM1.2-HR). J. Adv. Model. Earth Syst. 10, 1383–1413. https://doi.org/10.1029/2017MS001217.

Nash, J., Sutcliffe, J., 1970. River flow forecasting through conceptual models part I – A discussion of principles. J. Hydrol. 10, 282–290. https://doi.org/10.1080/00750770109555783.

Ndhlovu, G., Woyessa, Y., 2021. Evaluation of streamflow under climate change in the zambezi river basin of southern africa. Water 13, 10.3390/ w13213114.

Neitsch, S., Arnold, J., Kiniry, J., Williams, J., 2011. Soil & Water Assessment Tool Theoretical Documentation Version 2009. Texas Water Resources Institute 1–647. https://doi.org/10.1016/j.scitotenv.2015.11.063.

Nilawar, A.P., Waikar, M.L., 2019. Impacts of climate change on streamflow and sediment concentration under RCP 4.5 and 8.5: A case study in Purna river basin, India. Sci. Total Environ. 650, 2685–2696. https://doi.org/10.1016/j.scitotenv.2018.09.334.

Nyatuame, M., Amekudzi, L., Agodzo, S., 2020. Assessing the land use/land cover and climate change impact on water balance on tordzie watershed. Remote Sens. Appl.: Soc. Environ. 20, 100381 https://doi.org/10.1016/j.rsase.2020.100381.

O'Neill, B., Kriegler, E., Ebi, K., Kemp-Benedict, E., Riahi, K., Rothman, D., van Ruijven, B., van Vuuren, D., Birkmann, J., Kok, K., Levy, M., Solecki, W., 2017. The roads ahead: Narratives for shared socioeconomic pathways describing world futures in the 21st century. Global Environmental Change 42, 169–180. https://doi.org/10.1016/j.gloenvcha.2015.01.004.

OTB, 2018. OrfeoToolBox. Available online:https://www.orfeo-toolbox.org. (accessed on 23 July 2021).

Peres, D., Senatore, A., Nanni, P., Cancelliere, A., Mendicino, G., Bonaccorso, B., 2020. Evaluation of EURO-CORDEX (Coordinated Regional Climate Downscaling Experiment for the Euro-Mediterranean area) historical simulations by high-quality observational datasets in southern Italy: Insights on drought assessment. Natural Hazards Earth Syst. Sci. 20, 3057–3082. https://doi.org/10.5194/nhess-20-3057-2020.

Pravema, D., 2012. PROJECT Related to actions of the Phidias Foundation corresponding to Pravema activity 1. Technical Report.

Priestley, C., Taylor, R., 1972. On the assessment of surface heat flux and evaporation using large-scale parameters. Mon. Weather Rev. 100, 81–92.

Pulido-Velazquez, D., Collados-Lara, A., Pérez-Sánchez, J., Segura-Méndez, F., Senent-Aparicio, J., 2021. Climate change impacts on the streamflow in spanish basins monitored under near-natural conditions. J. Hydrol.: Regional Stud. 38, 100937 https://doi.org/10.1016/j.ejrh.2021.100937.

QGIS Development Team, 2021. QGIS Geographic Information System. Open Source Geospatial Foundation. Available online:http://qgis.osgeo.org. (accessed on 13 October 2021).

Quansah, J., Naliaka, A., Fall, S., Ankumah, R., El Afandi, G., 2021. Assessing future impacts of climate change on streamflow within the alabama river basin. Climate 9, 1–19. https://doi.org/10.3390/cli9040055.

R Core Team, 2020. R: A language and environment for statistical computing. R Foundation for Statistical Computing, Vienna, Austria. Available online:https://www.r-project.org. (accessed on 13 October 2021).

Raju, K., Kumar, D., 2020. Review of approaches for selection and ensembling of GCMS. J. Water Climate Change 11, 577–599. https://doi.org/10.2166/wcc.2020.128.

Rathjens, H., Bieger, K., Srinivasan, R., Arnold, J.G., 2016. CMhyd User Manual Documentation for preparing simulated climate change data for hydrologic impact studies. Technical Report.

Saade, J., Atieh, M., Ghanimeh, S., Golmohammadi, G., 2021. Modeling Impact of Climate Change on Surface Water Availability Using SWAT Model in a Semi-Arid Basin: Case of El Kalb River. Lebanon, Hydrology, p. 8.

Samuelsson, P., Gollvik, S., Kupiainen, M., Kourzeneva, E., van de Berg, W., 2015. The Surface Processes of the Rossby Centre Regional Atmospheric Climate Model (RCA4). Technical Report.

Sinan, M., Belhouji, A., 2016. Impact of the Climate Change on the climate and the water resources of Morocco on horizons 2020, 2050 and 2080 and measures of adaptation. La Houille Blanche 102, 32–39. https://doi.org/10.1051/lhb/2016037.

Skamarock, W., Klemp, J.B., Dudhia, J., Gill, D., Barker, D., Duda, M., Powers, J., 2008. A Description of the Advanced Research WRF Version 3. In: Technical Report, No. NCAR/TN-475+STR. University Corporation for Atmospheric Research, 10.5065/D68S4MVH.

von Storch, J.S., Putrasahan, D., Lohmann, K., Gutjahr, O., Jungclaus, J., Bittner, M., Haak, H., Wieners, K.H., Giorgetta, M., Reick, C., Esch, M., Gayler, V., de Vrese, P., Raddatz, T., Mauritsen, T., Behrens, J., Brovkin, V., Claussen, M., Crueger, T., Fast, I., Fiedler, S., Hagemann, S., Hohenegger, C., Jahns, T., Kloster, S., Kinne, S., Lasslop, G., Kornblueh, L., Marotzke, J., Matei, D., Meraner, K., Mikolajewicz, U., Modali, K., Müller, W., Nabel, J., Notz, D., Peters-von Gehlen, K., Pincus, R., Pohlmann, H., Pongratz, J., Rast, S., Schmidt, H., Schnur, R., Schulzweida, U., Six, K., Stevens, B., Voigt, A., Roeckner, E., 2017. MPI-M MPIESM1.2-HR model output prepared for CMIP6 HighResMIP. Earth System Grid Federation. Technical Report. 10.22033/ESGF/CMIP6.762.

Strandberg, G., Bärring, L., Hansson, U., Jansson, C., Jones, C., Kjellström, E., Kolax, M., M., K., Nikulin, G., Samuelsson, P., Ullerstig, A., Wang, S., 2014. CORDEX scenarios for Europe from the Rossby Centre regional climate model RCA4. Rep. Meteorol. Climatol. 116, 1–84.

Taia, S., Erraioui, L., Arjdal, Y., Chao, J., El Mansouri, B., Scozzari, A., 2023. The application of swat model and remotely sensed products to characterize the dynamic of streamflow and snow in a mountainous watershed in the high atlas. Sensors 23, 1246.

Taia, S., Erraioui, L., Mbrenga, N., Chao, J., El Mansouri, B., Haida, S., Taj-Eddine, K., 2021. Assessment of soil erosion using two spatial approaches: Rusle and swat model. E3S Web of Conferences 234, 1–7.

Tebaldi, C., Knutti, R., 2007. The use of the multi-model ensemble in probabilistic climate projections. Philos. Trans. R. Soc. A: Math., Phys. Eng. Sci. 365, 2053–2075. https://doi.org/10.1098/rsta.2007.2076.

Teutschbein, C., Seibert, J., 2012. Bias correction of regional climate model simulations for hydrological climate-change impact studies: Review and evaluation of different methods. J. Hydrol. 456–457, 12–29. https://doi.org/10.1016/j.jhydrol.2012.05.052.

Toreti, A., Bavera, D., Cammalleri, C., Cota, T., De Jager, A., Deus, R., Di Ciollo, C., Maetens, W., Magni, D., Masante, D., Mazzeschi, M., Mccormick, N., Cabrinha Pires, V., Quadrado, M., Saramago, M., Spinoni, J., 2022. Drought in western Mediterranean February 2022. Publications Office of the European Union, Luxembourg, Technical Report, 10.2760/927611.

Tramblay, Y., Jarlan, L., Hanich, L., Somot, S., 2018. Future scenarios of surface water resources availability in north african dams. Water Resour. Manage 32, 1291–1306.

Tramblay, Y., Ruelland, D., Somot, S., Bouaicha, R., Servat, E., 2013. High-resolution Med-CORDEX regional climate model simulations for hydrological impact studies: A first evaluation of the ALADIN-Climate model in Morocco. Hydrol. Earth Syst. Sci. 17, 3721–3739. https://doi.org/10.5194/hess-17-3721-2013.

Tuel, A., Kang, S., Eltahir, E., 2021. Understanding climate change over the southwestern Mediterranean using high-resolution simulations. Clim. Dyn. 56, 985–1001. https://doi.org/10.1007/s00382-020-05516-8.

UNECE, 2021. Environmental performance reviews, Morocco (second review). Technical Report, United Nations Economic Commission for Europe.

van den Hurk, B., Hewitt, C.D., Jacob, D., Bessembinder, J., Doblas-Reyes, F., Döscher, R., 2018. The match between climate services demands and earth system models supplies. Climate Services 12, 59–63. https://doi.org/10.1016/j.cliser.2018.11.002.

Verner, D., Treguer, D., Redwood, J., Christensen, J., McDonnell, R., Elbert, C., Konishi, Y., Belghazi, S., 2018. Climate Variability, Drought, and Drought Management in Morocco's Agricultural Sector. Technical Report.

van Vuuren, D., Edmonds, J., Kainuma, M., Riahi, K., Thomson, A., Hibbard, K., Hurtt, G., Kram, T., Krey, V., Lamarque, J.F., Masui, T., Meinshausen, M., Nakicenovic, N., Smith, S., 2011. K.R.S. The representative concentration pathways: An overview. Climatic Change 109, 5–31. https://doi.org/10.1007/s10584-011-0148-z.

Yin, J., Yuan, Z., Yan, D., Yang, Z., Wang, Y., 2018. Addressing climate change impacts on streamflow in the jinsha river basin based on cmip5 climate models. Water 10. https://doi.org/10.3390/w10070910.

Zhu, X., Ji, Z., Wen, X., Lee, S., Wei, Z., Zheng, Z., Dong, W., 2021. Historical and projected climate change over three major river basins in china from fifth and sixth coupled model intercomparison project models. Int. J. Climatol. 41 https://doi.org/10.1002/joc.7206.

Zhu, Y.Y., Yang, S., 2020. Evaluation of cmip6 for historical temperature and precipitation over the tibetan plateau and its comparison with cmip5. Adv. Climate Change Res. 11, 239–251.